

A Covariant, Chirally Symmetric, Confining Model of Mesons

Franz Gross

Department of Physics, College of William & Mary

Williamsburg, VA 23185

and

Continuous Electron Beam Accelerator Facility

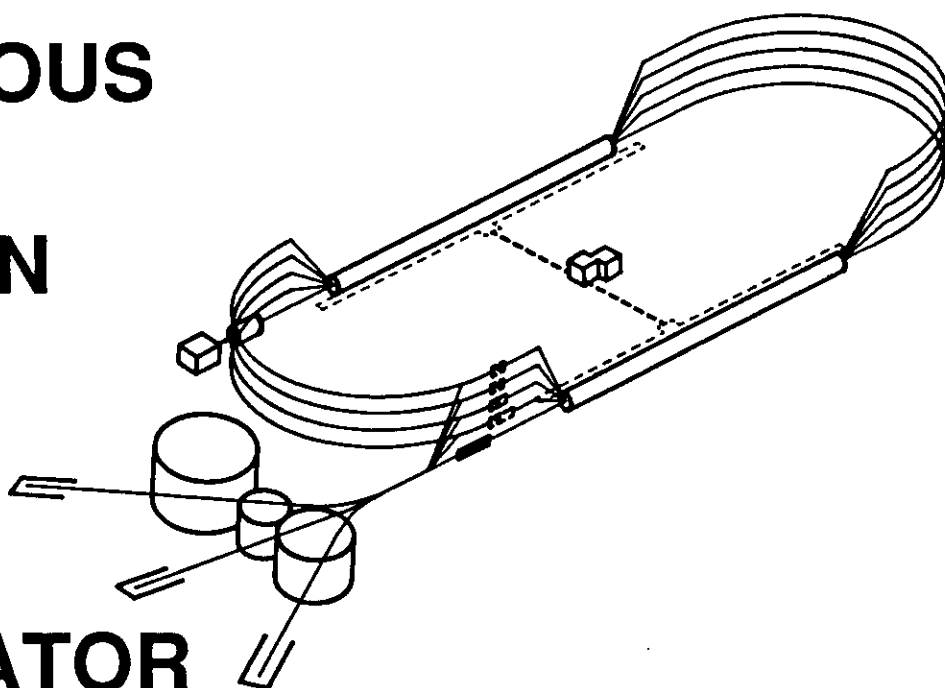
Newport News, VA 23606

Joseph Milana

Department of Physics, College of William & Mary

Williamsburg, VA 23185

CONTINUOUS ELECTRON BEAM ACCELERATOR FACILITY



SURA *Southeastern Universities Research Association*

CEBAF

The Continuous Electron Beam Accelerator Facility

Newport News, Virginia

Copies available from:

Library
CEBAF
12000 Jefferson Avenue
Newport News
Virginia 23606

The Southeastern Universities Research Association (SURA) operates the Continuous Electron Beam Accelerator Facility for the United States Department of Energy under contract DE-AC05-84ER40150.

DISCLAIMER

This report was prepared as an account of work sponsored by the United States government. Neither the United States nor the United States Department of Energy, nor any of their employees, makes any warranty, express or implied, or assumes any legal liability or responsibility for the accuracy, completeness, or usefulness of any information, apparatus, product, or process disclosed, or represents that its use would not infringe privately owned rights. Reference herein to any specific commercial product, process, or service by trade name, mark, manufacturer, or otherwise, does not necessarily constitute or imply its endorsement, recommendation, or favoring by the United States government or any agency thereof. The views and opinions of authors expressed herein do not necessarily state or reflect those of the United States government or any agency thereof.

A Covariant, Chirally Symmetric, Confining Model of Mesons

Franz Gross

Department of Physics, College of William & Mary, Williamsburg, VA. 23185
and
Physics Division, CEBAF, Newport News, VA. 23606

Joseph Milana

Department of Physics, College of William & Mary, Williamsburg, VA. 23185

Abstract: We introduce a new model of mesons as quark-antiquark bound states. The model is covariant, confining, and chirally symmetric. Our equations give an analytic solution for a zero mass pseudoscalar bound state in the case of exact chiral symmetry, and also reduce to the familiar, highly successful nonrelativistic linear potential models in the limit of heavy quark mass and lightly bound systems. In this fashion we are constructing a unified description of all the mesons from the pion through the upsilon. Numerical solutions for other cases are also presented.

1. Introduction

An important component of the CEBAF experimental program will be devoted to a detailed study of the quark structure of nucleons and baryon resonances, and to a search for signatures of the effect of these underlying quark degrees of freedom on nuclear structure. While there may be "smoking gun" signatures for such effects which depend only on the comparatively easily understood perturbative features of QCD,¹ a thorough understanding of baryon and nuclear structure at the momentum transfers available at CEBAF must also take the non-perturbative aspects of QCD into account. A careful treatment of confinement is therefore essential to such a study.

Many models (the various bag models,²⁻¹³ flip-flop models,¹⁴ and non-relativistic potential models¹⁵) already exist and have proven useful in this context, and will continue to do so. However, one notable characteristic of all of the most popular models presently used is that they do not describe bound states in a Lorentz covariant fashion. While this may not be a serious limitation in the treatment of inclusive processes, such as inelastic electron scattering,¹⁶ in which one is probing the properties of a static target nucleus, it is a serious handicap when describing exclusive or semi-exclusive events, in which a particular hadron is to be observed in the final state. For these processes, which will clearly play a large part in the experimental program carried out at the new accelerators, it is essential to have a framework in which the quark-gluon bound states can be treated covariantly.

The goal of this paper, which we expect to be the first in a series, is to develop a technique for modeling confinement which is consistent with chiral symmetry and which also is exactly covariant. We believe that both of these requirements (exact covariance and consistency with chiral symmetry) are essential if the results of such models are to be expected to have any real predictive power. Even at CEBAF energies and momentum transfers, mesons and nucleons recoil at relativistic velocities, and we must be able to describe such a simple process correctly. Furthermore, we believe that the equations should also conserve angular momentum exactly, as this is still an important constraint at these energies. And a proper treatment of the pion, essential for nuclear physics applications, cannot be expected unless the implications of chiral symmetry are built in from the start. The model introduced in this paper has been developed with all of these

requirements in mind, and is, to our knowledge, the first time chiral symmetry, confinement, and exact covariance have been combined in a single, solvable model. [However, see Refs. 17-19 for a model in which chiral symmetry and confinement are built in through an instantaneous, and hence noncovariant, potential.]

As a demonstration of the workability of our method, we show in this paper how it can be used to study the structure of mesons. In later work we plan to add one gluon exchange (OGE), do a systematic study of the meson spectrum, and eventually apply the method to the study of baryons and simple nuclear systems.

The following features have been incorporated into the model:

(i) Mesons are viewed as bound states of two constituent quarks that can be off-shell. In this sense, our model is a simple generalization of the non-relativistic (or semi-relativistic) models of Isgur and his collaborators,¹⁵ but the relativistic propagation of off-shell quarks includes some additional contributions from q - q bar pairs. The success of these models in describing the meson spectrum encourages us to believe that we will also be able to eventually describe the meson spectrum successfully.

(ii) Exact covariance is achieved by working in momentum space, where non-localities and energy dependences can be treated comparatively easily.

(iii) The confining potential is made up of a constant part, which permits us to adjust the overall energy scale, plus a relativistic generalization of the linear part known to emerge, in the quenched approximation, from lattice gauge calculations.²⁰ In particular, the potential is constructed from a "leading" q^{-4} term, regularized by subtracting the leading singularity at $q^2 = 0$. The form of the potential is derived directly from a consideration of the non-relativistic linear potential in momentum space, as discussed in Sec. 2.

(iv) The spin dependent structure of the confining potential is chosen to be consistent with chiral symmetry. [In this first paper we explore the simplest case of chiral symmetry under the $U(1) \times U(1)$ group. This still gives a large number of possibilities, and the best choice, together with extension to the more realistic $SU(2) \times SU(2)$ case, will be deferred to a later work in which we fit the meson

spectrum.] We assume, in the spirit of the Nambu Jonas-Lasinio (NJL) model,²¹ that the symmetry is spontaneously broken, giving the quark a constituent mass which arises dynamically from its self interaction with the confining forces. The pion then emerges naturally as the Goldstone boson associated with this dynamical symmetry breaking, and its non-zero mass also emerges as a natural consequence of the symmetry breaking introduced by the small bare quark mass term in the QCD Lagrangian. This is discussed in Sec. 3 and further in Sec. 4.

The relativistic bound state equations we introduce have the feature that the relative energy variable is constrained by restricting the quark to its positive energy mass shell (referred to as the one-channel case), or, in the case of very deeply bound states, including two channels, one with the *quark* on its *positive* energy mass shell and one with the *antiquark* on its *negative* energy mass shell. [We will show in Secs. 4 and 5 that the second channel is very small unless the binding is very strong or the quarks are very light, so that for weakly bound, heavy quark systems the one-channel case can legitimately be considered as an excellent approximation to the more correct two-channel case.] This feature means that even though the equations are exactly covariant, they depend, like non-relativistic equations, on the relative three-momentum only, and have a smooth non-relativistic limit. The one-channel version of these equations has been used extensively for the study of few-nucleon systems in the context of relativistic meson theory,²² and the two-channel version was briefly discussed previously,²³ but this is, to our knowledge, the first time these equations have been applied to the study of quark bound states, and also the first time it has been demonstrated that deeply bound states can be successfully described in this manner.

There are a number of justifications for using a relativistic equation in which the (heavy) constituents are restricted to their mass shell. In the context of relativistic meson theory, it can be shown²⁴ that (a) the infinite sum of all ladder and crossed ladder exchange diagrams is necessary in order to derive a one body equation for a (light) particle (moving in an instantaneous potential created by a spinless heavy particle) in the limit when the mass of the heavy particle approaches infinity, and (b) the two body equation which sums this series efficiently in the same limit is *not* the Bethe-Salpeter equation, but one in which the heavy particle is restricted to its mass shell. Briefly, the reason for this result is that the

parts of the ladder diagrams in which *both* constituents are off-shell tend to cancel the crossed ladder diagrams, leaving only the parts of the ladder diagrams in which the heavy constituent is on-shell. This happens in *all* orders, and in some theories the cancellation is *exact* as the heavy constituent mass approaches infinity.

It may seem strange (or even incorrect!) to treat confined quarks as on-shell particles. In response to this anticipated objection, we offer the following:

(i) Confinement in our model arises from the linear interaction *between neighboring quarks* in a color singlet; the dynamical mass of such a confined quark is *finite*. We do not offer a method for the calculation of the self energy of an isolated quark, and in this sense our method is complementary (or orthogonal) to that developed by Roberts *et. al.*²⁵

(ii) Since the self energy of the confined quark is finite, its propagator has the usual form, and because the singularities which arise from the confining q^4 terms are "softened" by regularizing subtractions [see item (iii) above and the discussion in Sec. 4] the poles of the quark propagators are the dominant singularities, leading to the equations we use.

(iii) The structure of the one-channel equation insures that the OGE terms, when added later, will be color gauge invariant. We have not yet proved that this is also true of the two-channel equation, but expect it to be so.

(iv) Putting quarks on-shell is consistent with both non-relativistic theory and the commonly used light-front formalism, where it is assumed that *all* quarks and gluons are on mass-shell.

One of the limitations of the present work is that the quark self energies in the bound state equations have been approximated by constants, and have therefore not been treated in a fully self consistent manner. The method of restricting quarks (or antiquarks) to their mass shell makes it easier to carry out such a completely self consistent program, and this is planned for a subsequent work. Preliminary results suggest that these effects may lead to corrections as large as 50%.

The paper is organized into six sections and one appendix. In Sec. 2 we define the

linear potential in momentum space, and introduce the one-channel equation. Section 3 discusses how we use the ideas of the NJL model to treat chiral symmetry, and shows how the pion emerges as the Goldstone boson. Section 4 then combines the results of the two previous sections, emerging with relativistic two-channel equations consistent with chiral symmetry. Numerical solutions of both the one-channel and two-channel equations are obtained and discussed in Sec. 5. Some conclusions are given in Sec. 6. The appendix contains some technical issues concerning the regularization of our confining potential.

2. The Linear Potential

A relativistic treatment is most conveniently carried out in momentum space, where non-localities are easily handled. This requires that the linear confining potential be treated in momentum space also, and in this section the details of how this has been done are presented.

2.1 Non-relativistic case

To treat the non-relativistic problem it is convenient to start with the relation

$$V(r) = \sigma r = \lim_{\epsilon \rightarrow 0} \sigma r e^{-\epsilon r} = \lim_{\epsilon \rightarrow 0} \sigma \frac{d^2}{d\epsilon^2} \left(\frac{e^{-\epsilon r}}{r} \right) . \quad (2.1)$$

The potential in momentum space becomes

$$V(q) = \int d^3r e^{i\mathbf{q} \cdot \mathbf{r}} V(r) = \sigma \lim_{\epsilon \rightarrow 0} \frac{d^2}{d\epsilon^2} \left(\frac{4\pi}{q^2 + \epsilon^2} \right) \quad (a)$$

$$= 8\pi \sigma \lim_{\epsilon \rightarrow 0} \left[-\frac{1}{(q^2 + \epsilon^2)^2} + \frac{4\epsilon^2}{(q^2 + \epsilon^2)^3} \right] \quad (b)$$

$$= \lim_{\epsilon \rightarrow 0} \left[V_A(q) + \frac{32\pi \sigma \epsilon^2}{(q^2 + \epsilon^2)^3} \right] \quad (c) \quad (2.2)$$

where V_A is defined through the last equation. At this point it is tempting to let $\varepsilon \rightarrow 0$, and to obtain the result that the linear potential in momentum space is simply $V_A(q)$. However this is inadequate because the resulting q^{-4} potential is very singular at $q = 0$, and does not even describe the original linear potential. To see this, it is useful to recall that the linear potential (2.1) is zero at $r = 0$, and therefore

$$\int \frac{d^3 q}{(2\pi)^3} V(q) = 0 \quad (2.3)$$

This condition is satisfied by the exact result (2.2b), but is not satisfied by V_A . Explicitly,

$$\begin{aligned} V_A(r) &= \int \frac{d^3 q}{(2\pi)^3} e^{-i q \cdot r} V_A(q) = -\sigma \frac{e^{-\varepsilon r}}{\varepsilon} \\ &\xrightarrow{\varepsilon \rightarrow 0} \sigma \left[r - \frac{1}{\varepsilon} \right] \end{aligned} \quad (2.4)$$

showing that V_A approaches an infinitely large negative value as $\varepsilon \rightarrow 0$. The additional term in (2.2c) "corrects" (2.4) by supplying the (infinite) constant needed to normalize the potential to zero at the origin. However, it has an inconvenient form, because as $\varepsilon \rightarrow 0$ it is small everywhere except at $q^2 = 0$, where it is singular. In fact it behaves somewhat like a delta function, and since its role is merely to cancel the infinite constant in (2.4), we are lead to an alternative definition of the linear potential

$$V_L(q) \equiv \lim_{\varepsilon \rightarrow 0} \left[V_A(q) - \delta^3(q) \int d^3 q' V_A(q') \right] \quad (2.5)$$

This potential satisfies the condition (2.3) identically, and its Fourier transform is

$$V_L(r) = \lim_{\varepsilon \rightarrow 0} \left[-\sigma \frac{e^{-\varepsilon r}}{\varepsilon} + \frac{\sigma}{\varepsilon} \right] \xrightarrow{\varepsilon \rightarrow 0} \sigma r \quad (2.6)$$

For finite ε , this potential is not identical to the original model (2.1), but has the same limit as $\varepsilon \rightarrow 0$, and is therefore an equally good choice.

To adjust the mass scale, a constant term is often added. In momentum space this corresponds to:

$$V_C(q) = (2\pi)^3 \delta(q) m_R C \quad (2.7)$$

where m_R is the reduced mass of the $q \bar{q}$ system, and C is a dimensionless constant. The total potential, V_T is then the sum of V_L and V_C .

The potential can now be inserted into a Schrödinger equation, which in momentum space takes the form

$$\begin{aligned} \left(\frac{p^2}{2m_R} - E \right) \Psi(p) &= - \int \frac{d^3 k}{(2\pi)^3} V_T(\mathbf{p} - \mathbf{k}) \Psi(k) \\ &= - \lim_{\varepsilon \rightarrow 0} \int \frac{d^3 k}{(2\pi)^3} V_A(\mathbf{p} - \mathbf{k}) [\Psi(k) - \Psi(p)] + m_R C \Psi(p) \\ &= 8\pi\sigma \int \frac{d^3 k}{(2\pi)^3} \frac{[\Psi(k) - \Psi(p)]}{(\mathbf{p} - \mathbf{k})^4} + m_R C \Psi(p) \end{aligned} \quad (2.8a)$$

where \mathbf{p} and \mathbf{k} are the outgoing and incoming momenta of the quark to which a momentum $\mathbf{q} = \mathbf{p} - \mathbf{k}$ is transferred. Note that the $\varepsilon \rightarrow 0$ limit can actually be taken in the last step in (2.8a), because the wave function subtraction, $[\Psi(k) - \Psi(p)]$, cancels the strong singularity at $p = k$, insuring that the integral on the RHS is finite. It is important to be able to take this limit, because the quarks are *truly confined* by the linear potential *only* when $\varepsilon = 0$. This can be seen by examining (2.6) and (2.8a) in position space. For finite ε , the potential approaches $1/\varepsilon$ as $r \rightarrow \infty$, so that quarks with energies $E > 1/\varepsilon + C$ can escape to infinity. This is the principal reason for preferring the form (2.5) to that of (2.2c).

The nonrelativistic linear potential is scale invariant, and therefore the reduced quark

mass can be scaled out of the Eq. (2.8a) by introducing dimensionless momenta $p_o = p/m_R$ and $k_o = k/m_R$, giving

$$\left(\frac{1}{2} p_o^2 - E_o\right) \Psi(p_o) = 8\pi \left(\frac{\sigma}{m_R^2}\right) \int \frac{d^3 k_o}{(2\pi)^3} \frac{[\Psi(k_o) - \Psi(p_o)]}{(p_o - k_o)^4} + C \Psi(p_o) \quad (2.8b)$$

The form of (2.8b) shows explicitly that the energy $E = m_R E_o$ depends on two dimensionless numbers: $\sigma_o = \sigma/m_R^2$ and C .

In order to test our progress thus far, we solve equation (2.8) for the ground state energy and compare with the exact solution

$$E = m_R \left[C + 2.33 \left(\frac{1}{2} \sigma_o^2 \right)^{\frac{1}{3}} \right] \quad (2.9)$$

where 2.33 is the location of the first node of the Airy function. [The $\ell=0$, S wave solutions to the Schrodinger equation for a linear potential in position space are well known to be given simply by the Airy functions. Solving the fourier transformed, integral equation, (2.8), is however a more formidable task.] Our numerical method, described in detail in Sec. 5 below, converges quickly to this correct value, as illustrated in Table 1. The wave function also agrees with the non-relativistic result.

For applications to the relativistic problem, it is convenient to have a simple way to estimate the eigenvalues expected, and this is provided by Feynman's famous trick²⁶ using the uncertainty relation. Taking ground state expectation values of (2.8), and using the uncertainty relation to replace $\langle p_o \rangle$ by $\langle 1/m_R r \rangle$, gives

$$E = m_R \left[C + \frac{1}{2} \left(\frac{1}{r_o} \right)^2 + \sigma_o r_o \right] \quad (2.10)$$

where $r_o = \langle m_R r \rangle$. Minimizing this expression with respect to r_o gives

$$r_o = \left(\frac{1}{\sigma_o} \right)^{\frac{1}{3}}, \quad E = m_R \left[C + \frac{3}{2} (\sigma_o^2)^{\frac{1}{3}} \right] \quad (2.11)$$

which is remarkably close to the exact value.

2.2 Relativistic case

The previous discussion will now be generalized to relativistic systems. To motivate the development, systems with at least one massive quark will be discussed first, followed, in this section, by only a few comments on light quark systems. More discussion of light quark systems will be given in Sec. 5, but a complete treatment of these systems is postponed for a later paper.

The obvious way to generalize the definition (2.5) is to replace the non-relativistic q^2 by the relativistic $q^2 = q_0^2 - \mathbf{q}^2$. If one of the two quarks is massive, the energy transferred to it, q_0 , is expected to be small, so that the nonrelativistic limit should emerge as the quark mass approaches infinity. However, this physical limit will not emerge naturally unless some care is taken with the treatment of q_0 . [Recall the discussion of this point in the Introduction.] One way to maintain covariance exactly, but also to allow the non-relativistic limit to emerge naturally, is to restrict the heavy quark to its mass shell, so that the four momentum transfer becomes

$$q^2 = (E_p - E_k)^2 - (\mathbf{p} - \mathbf{k})^2, \quad E_p = \sqrt{m_1^2 + p^2} \quad (2.12)$$

where m_1 is the mass of the heavy quark. The energy transfer now automatically approaches zero as $m_1 \rightarrow \infty$.

This "potential" can be treated consistently to all orders if it is taken to be the kernel of a relativistic equation in which the heavy quark is restricted to its mass shell throughout. For spin $1/2$ particles, the kernel will be written in the form

$$V_{12}(p, k; P) = V_{eff}(p, k; P) \sum_i O_1^i O_2^i \quad (2.13)$$

where the Dirac matrices O which operate on the Dirac indices of particles 1 and 2 describe the spin dependent structure of the kernel, and V_{eff} , a covariant scalar function, gives the momentum dependence of the effective confining potential. The four momentum variables are related to the momenta of the quark, p_1 , and the antiquark, p_2 , by

$$\begin{aligned} p_1 &= \frac{1}{2}P + p & P &= p_1 - p_2 \\ p_2 &= p - \frac{1}{2}P & p &= \frac{1}{2}(p_1 + p_2) \end{aligned} \quad (2.14)$$

with the direction of the antiquark momenta as shown in Fig. 2 (Sec. 3). The spin structure of the kernel will be discussed in Sec. 3; the form of V_{eff} will be discussed here.

The relativistic equation which uses the kernel (2.13), with the quark on mass-shell, has the form

$$\Gamma(p, P) = - \int \frac{d^3 k}{(2\pi)^3 2E_k} \frac{V_{eff}(p, k; P)}{(m_2^2 - k_2^2)} \sum_i O_i [m_1 + \not{p}_1] \Gamma(k, P) [m_2 + \not{p}_2] O_i \quad (2.15)$$

where Γ is the bound state vertex function. The covariance of (2.15) is obvious if the integration is expressed in its equivalent covariant form:

$$\int \frac{d^3 k}{2E_k} = \int d^4 k \delta_+(m_1^2 - k_1^2) \quad (2.16)$$

Many choices of the O 's consistent with chiral symmetry are possible, and are discussed in Sec. 3. The choice we will make there has the property

$$\sum_i O_i [m_1 + \not{p}_1] \gamma^5 [m_2 + \not{p}_2] O_i = 2(m_1 m_2 - k_1 \cdot k_2) \gamma^5, \quad (2.17)$$

which means that the pseudoscalar solutions of (2.15) have a pure γ^5 structure:

$$\Gamma(p, P) = \Gamma_0(p, P) \gamma^5 \quad (2.18)$$

Specifically, substituting the ansatz (2.18) into (2.15) and using (2.17) gives the following equation for the scalar function Γ_0

$$\begin{aligned} \Gamma_0(p, P) &= - \int \frac{d^3 k}{(2\pi)^3 E_k} \frac{[m_1 m_2 - k_1 \cdot k_2]}{(m_2^2 - k_2^2)} V_{eff}(p, k; P) \Gamma_0(k, P) \\ &= - \int \frac{d^3 k}{(2\pi)^3} V_{eff}(p, k; P) \frac{\Gamma_0(k, P)}{2E_k - \mu} \end{aligned} \quad \begin{matrix} (a) \\ (b) \end{matrix} \quad (2.19)$$

where (2.19b) holds if $m_1 = m_2$, and $P = (\mu, \mathbf{0})$, which will be assumed for the remainder of the discussion.

The function V_{eff} is now constructed by following steps which parallel the construction of its non-relativistic counterpart, Eq. (2.5). We require each step in the construction to be manifestly covariant, and to reduce, in the limit as $m_1 \rightarrow \infty$, to the corresponding step in the construction of (2.5). There were two principal steps leading to (2.5): (i) the definition of $V_A(q)$, and (ii) the regularization of its singular behavior at $q = 0$ by the imposition of the constraint (2.3). We have already discussed the relativistic generalization of $V_A(q)$; the straightforward replacement of q^2 by $-q^2$, where q^2 was defined in Eq. (2.12), satisfies the two requirements of covariance and smooth approach to the non-relativistic limit. The second step is also straightforward if (2.16) is used to recast the constraint into a covariant form

$$\int \frac{d^3 k}{(2\pi)^3} \left(\frac{m}{E_k} \right) V(p, k; P) = 0 \quad (2.20)$$

[Because V is no longer local, (2.20) it is conveniently expressed as an integral over the momentum of the incoming, on-shell, quark. We could just as well integrate over the

momentum of the on-shell outgoing quark.] Following the principle that the subtraction which cancels the singularities in V and impliments the constraint (2.20) should be in the form of a δ function, with support in the region where V is singular, and adding a "constant" potential which is the relativistic generalization of (2.7), gives the following form for V_{eff}

$$V_{eff}(p, k; P) = V_{RA}(p, k) - E_k \delta(p - k) \int \frac{d^3 k'}{E_{k'}} V_{RA}(p, k') + C (2\pi)^3 E_k \delta(p - k) \quad (2.21)$$

Unfortunately, the term V_{RA} must include a cutoff factor (or form factor) not needed in its non-relativistic counterpart, V_A , because, without such a factor the integral in (2.21) will not converge at large k' . We take

$$V_{RA}(p, k) = -8\pi\sigma \left[\frac{1}{q^4} - \frac{1}{\Lambda^4 + q^4} \right] \quad (2.22)$$

with q^2 defined in Eq. (2.12).

The relativistic equation and relativistic linear potential for heavy quark systems are now completely defined. Substituting (2.21) into (2.19b) gives

$$(2E_p - \mu + E_p C) \Psi(p) = - \int \frac{d^3 k}{(2\pi)^3} V_{RA}(p, k) \left[\Psi(k) - \left(\frac{E_p}{E_k} \right) \Psi(p) \right] \quad (2.23)$$

where the wave function is

$$\Psi(p) = \frac{\Gamma_0(p, P)}{(2E_p - \mu)} \quad (2.24)$$

Note that Eq. (2.23) reduces to the Schrödinger Eq. (2.8) in the limit $m \rightarrow \infty$, provided

that $\Lambda \rightarrow \infty$ also, and that $\mu = 2m + E$ and $2m_R = m$.

The q^{-4} term in the relativistic kernel still scales with the quark mass, but the form factor mass Λ spoils this scale invariance, unless it is restored by adopting the convention that this mass is also to be scaled by the quark mass:

$$\Lambda = m \Lambda_o \quad (2.25)$$

so that Λ_o (instead of Λ) is to be fixed. Since this scale invariance is an important feature of the linear potential we are modeling, and since the cutoff mass does not represent a scale of physical significance, we will adopt this convention, and chose a value of Λ_o which insures that the relativistic kernel approximates the behavior of a linear potential as nearly as possible. [Since Λ_o is one of the parameters of our model, its final value will be determined in a later work from fits to the entire meson spectrum. In this paper, we chose $\Lambda_o = 1.7$, as discussed in Sec. 5.] With this choice, the dependence of the relativistic equation (2.23) on the quark mass can be scaled away just as was done for the nonrelativistic equation, and its solutions depend sensitively on the same two dimensionless parameters, σ_o and C .

Equation (2.23) forms the backbone of our covariant, relativistic confining model. However, to include the light mesons, and especially the pion, we still need to incorporate chiral symmetry and also extend our on-shell reduction, natural in the heavy quark limit, to that of the light quark case. These are done in Secs 3 and 4, respectively. Before proceeding to do so, we first wish to discuss the structure and solutions of equation (2.23) in a little more detail.

Two families of solutions are of particular interest. When $\sigma_o \ll 1$ and C is not too close to -2 , it follows that $p_o = \langle p \rangle / m \ll 1$, and the qualitative behavior of the solutions can be understood by expanding the equation in powers of m^{-1} :

$$\left(p_o^2 \left[1 + \frac{1}{2} C \right] + 2 - \mu_o + C \right) \Psi(r_o) = - \sigma_o r_o \Psi(r_o) \quad (2.26)$$

where now all quantities with a subscript o have been scaled by the quark mass. Using the uncertainty principle, this gives the following estimates for the size and mass of the

lowest bound state:

$$r_o = \left(\frac{2+C}{\sigma_o} \right)^{\frac{1}{3}}, \quad \mu = m \left[2+C+2 \left(\left[1+\frac{1}{2}C \right] \sigma_o^2 \right)^{\frac{1}{2}} \right] \quad (2.27)$$

Note that the *size and mass of the bound state are now correlated* through the constant C ; in particular, as $C \rightarrow -2$, the bound state mass and radius *both* approach zero. This behavior is not an artifact of the non-relativistic approximation; examination of the exact equation (2.23) shows that if $C = -2$, the solution is

$$\Psi(p) = \frac{N}{E_p} \quad (\text{for } \mu = 0) \quad (2.28)$$

where N is a constant. The slow fall-off of this function with p , the relativistic analogue of a constant, corresponds to a delta function in position space. In Sec. 5 we will see how we use this correlation with the constant C to get the pion, a nearly zero mass bound state, correctly, and we will show that the estimate (2.27) agrees quite well with the actual calculations.

3. Chiral Symmetry

As previously discussed, the goal of the model is a unified description of all the mesons, from the pion to charmonium and the other heavy quark systems. In the last section we saw how to generalize the nonrelativistic linear potential models known to successfully describe charmonium to a covariant setting. Such a step is clearly necessary in order to either deal with boosts or with the lighter quark systems. The pion, as the lightest of the mesons, and believed to be the Goldstone boson associated with the breaking of chiral symmetry of the QCD Lagrangian, must be addressed separately. As this involves a separate and independent line of development from that presented in Sec. 2, we will in this section drop the on-shell, three dimensional reduction made there and instead work in

the full, four dimensional Minkowski space. In Sec. 4 we will then merge, through various approximations, the results of the two sections and thus finally fully define our model.

In recent years the old theory of Nambu Jona-Lasinio (NJL)²¹ has been resurrected²⁷ as a possible model for the chiral symmetry breaking mechanism of QCD. Originally describing pions as bound states of nucleons, the theory has received a much more plausible application in the context of QCD as modeling the low-energy interactions of quarks. In NJL, chiral symmetry is dynamically broken through the self-interactions of the fermions. The existence of a deeply bound pseudoscalar state subsequently follows naturally. We adopt this approach and also assert that QCD breaks chiral symmetry dynamically. Since low-energy QCD certainly contains a lot of dynamics, such an approach appears quite natural. However, unlike NJL where the quarks only interact at a point and thus lose all information about the infrared structure of QCD, dynamical symmetry breaking is implemented within our potential approach. We are thus in effect generalizing NJL to include confinement.

Since we have no fundamental Lagrangian describing our potential, we work from analogy with NJL. The potential interaction of the quarks is modeled as an exchange interaction (as would occur in a simple boson exchange picture), involving two three point vertices with the exchanged momentum determined by energy-momentum conservation. The spinor structure of this interaction, O , is as yet undetermined. From general considerations it must be chirally symmetric, but not all such choices for O will yield a zero mass pion (in the case of zero bare quark mass). Nevertheless, there is still a large set $\{O^\pi\}$ that do, and the exact form of O^π will have to be deferred to a later work when we fit the entire meson spectrum.

Following NJL, consider the self-consistent (Hartree)-Fock equation for the two point Green's function at the one loop order, shown schematically in Fig. 1. Defining

$$\Sigma(p) = p\Sigma^*(p) + \Sigma'(p) \tag{3.1}$$

as the quark's self-energy, Fig. 1 gives:

$$p\Sigma^\nu(p) + \Sigma^\nu(p) = i \int \frac{d^4 k}{(2\pi)^4} V_{\mathcal{A}}(p-k) \sum_i O_i^\pi \frac{1}{(k - m_o - \Sigma(k))} O_i^\pi, \quad (3.2)$$

where m_o is the bare mass of the quark.

We next write down the bound state equation for two dynamical quarks using the ladder approximation, shown schematically in Fig. 2. As in NJL, we use the full quark propagator. Defining $\Gamma(p, P)$ as the vertex function, where P^2 is the invariant mass squared of the bound state, Fig. 2 gives:

$$\Gamma(p, P) = i \int \frac{d^4 k}{(2\pi)^4} V_{\mathcal{A}}(p-k) \sum_i O_i^\pi S(k + \frac{P}{2}) \Gamma(k, P) S(k - \frac{P}{2}) O_i^\pi, \quad (3.3)$$

where

$$S(q) = \frac{1}{(q - m_o - \Sigma(q))}. \quad (3.4)$$

We will now show how, with a particular choice of O^π , these equations are consistent with a zero mass pion bound state when m_o is zero. As a first example consider invariance under the $SU(2) \times SU(2)$ group, and take O^π so that

$$\sum_i O_i^\pi O_i^\pi = 1 - \gamma_1^5 \gamma_2^5 \tau_1 \tau_2, \quad (3.5)$$

i.e. the sum of scalar-isoscalar and pseudoscalar-isovector exchange terms. The self-energy equation then becomes:

$$\begin{aligned} \Sigma^\nu(p) &= -2i \int \frac{d^4 k}{(2\pi)^4} V_{\mathcal{A}}(p-k) \frac{(m_o + \Sigma^\nu(k))}{k^2(1 - \Sigma^\nu(k^2))^2 - (m_o + \Sigma^\nu(k))^2}, \\ p^2 \Sigma^\nu(p) &= 4i \int \frac{d^4 k}{(2\pi)^4} V_{\mathcal{A}}(p-k) \frac{p \cdot k(1 - \Sigma^\nu(k))}{k^2(1 - \Sigma^\nu(k^2))^2 - (m_o + \Sigma^\nu(k))^2}. \end{aligned} \quad (3.6)$$

With the same interaction, the bound state equation for a zero mass pion with a vertex

function of the form:

$$\Gamma(p, \mu) = \Gamma_o(p) \tau \gamma^5 \quad (3.7)$$

becomes

$$\begin{aligned} \Gamma_o(p) \tau \gamma^5 = i \tau \int \frac{d^4 k}{(2\pi)^4} \frac{V_{\mathcal{A}}(p-k)}{[k^2(1-\Sigma'(k^2))^2 - (m_o + \Sigma'(k^2))^2]^2} \times \\ \{ (k(1-\Sigma'(k^2) + m_o + \Sigma'(k^2)) \Gamma_o(p) \gamma^5 (k(1-\Sigma'(k^2) + m_o + \Sigma'(k^2)) + \\ \gamma^5 (k(1-\Sigma'(k^2) + m_o + \Sigma'(k^2)) \Gamma_o(p) \gamma^5 (k(1-\Sigma'(k^2) + m_o + \Sigma'(k^2)) \gamma^5 \} \end{aligned} \quad (3.8)$$

Passing all the γ^5 's to the left (as we have already done in the above with the τ 's) we get for $\Gamma_o(p)$

$$\Gamma_o(p) = -2i \int \frac{d^4 k}{(2\pi)^4} V_{\mathcal{A}}(p-k) \frac{\Gamma_o(k)}{k^2(1-\Sigma'(k^2))^2 - (m_o + \Sigma'(k))^2} . \quad (3.9)$$

Comparison of the self-energy and pion equations shows that, in the case of zero bare quark mass, $m_o=0$, the pion equation is insured of having a solution, namely

$$\Sigma'(p) = \Gamma_o(p) . \quad (3.10)$$

On the other hand, if $m_o \neq 0$, the pion equation is inconsistent with the self-energy equation. Hence, if $m_o=0$ there is a pion state with zero mass while if $m_o \neq 0$, there is no such state. We have thus generalized the mechanism of dynamical symmetry breaking of NJL from point-like quark interactions to interactions acting over an arbitrary distance and have thus incorporated in our model all the main qualitative features of low energy QCD, namely: chiral symmetry breaking and confinement.

The choice of O^{π} is not unique; other structures exist that will yield a zero mass pion solution when $m_o=0$. Interestingly, one structure invariant under the simplest chiral $U(1) \times U(1)$ group that does *not* have this property is the sum of scalar-isoscalar and pseudoscalar-isoscalar terms, *i.e.*

$$\sum_i O_i^\pi O_i^\pi = 1 - \gamma_1^5 \gamma_2^5 . \quad (3.11)$$

In this case there is no dynamical symmetry breaking and hence no zero mass pion state. With respect to the chiral $U(1) \times U(1)$ group, one structure for O^π which *does* give dynamical symmetry breaking is

$$\sum_i O_i^\pi O_i^\pi = \frac{1}{2} (1 - \gamma_1^5 \gamma_2^5 - v \gamma_1^\mu \gamma_{2\mu}) , \quad (3.12)$$

i.e. the sum of scalar, pseudoscalar and vector terms (all isoscalar) where v is an arbitrary, nonzero, constant. This form has the advantage of being independent of the quark flavor and will thus, perhaps, be a more natural choice for fitting the meson spectrum. However, in this case a more complicated structure for the vertex function is required in order to solve the pion equation, namely

$$\Gamma(p, P) = \Gamma_1(p, P) \tau \gamma^5 + \Gamma_2(p, P) \tau \gamma^5 P + \Gamma_3(p, P) \tau \gamma^5 p . \quad (3.13)$$

The equations for the vertex function greatly simplify if $v = 1$ and the form for $\Gamma(p, P)$ is then again given by Eq. (3.7). Because of this simplification we have chosen to use this particular form for O^π for the remainder of this first, introductory work. Again, the optimal form for O^π is part of our parameter fitting and the selection of a final form, together with the extension to the more realistic $SU(2) \times SU(2)$ group, will have to be deferred to a later work when we are fitting the physical mesons. For subsequent use in the next section, we now simply state our results for the self-energy and vertex function equations with this last ($v = 1$) form for O^π . For the quark self-energy we get:

$$\begin{aligned} \Sigma^s(p) &= -2i \int \frac{d^4 k}{(2\pi)^4} V_{\mathcal{A}}(p-k) \frac{m_o + \Sigma^s(k)}{k^2 (1 - \Sigma^v(k^2))^2 - (m_o + \Sigma^s(k))^2} , \\ p^2 \Sigma^v(p) &= 2i \int \frac{d^4 k}{(2\pi)^4} V_{\mathcal{A}}(p-k) \frac{p \cdot k (1 - \Sigma^v(k))}{k^2 (1 - \Sigma^v(k^2))^2 - (m_o + \Sigma^s(k))^2} . \end{aligned} \quad (3.14)$$

which is nearly identical to our earlier result, Eq. (3.6). The vertex equation becomes:

$$\Gamma_o(p) = -2i \int \frac{d^4 k}{(2\pi)^4} \frac{V_{eff}(p-k) \Gamma_o(k)}{D(+) D(-)} \left((k^2 - \frac{P^2}{4}) A(+) A(-) - B(+) B(-) \right), \quad (3.15)$$

where

$$\begin{aligned} A(\pm) &= 1 - \Sigma_v(k \pm \tfrac{1}{2}P), & B(\pm) &= m_o + \Sigma_s(k \pm \tfrac{1}{2}P), \\ D(\pm) &= (k \pm \tfrac{1}{2}P)^2 A(\pm)^2 - B(\pm)^2. \end{aligned} \quad (3.16)$$

Once again, if the pion mass is zero and m_o is zero, the equation for $\Gamma_o(p)$ reduces identically to that for the scalar self-energy, $\Sigma^S(p)$.

We must now discuss how the potential $V_{eff}(p-q)$ appearing in equations (3.14) and (3.15) is defined and thus wed the results of this section with that of Sec. 2. This brings us to Sec. 4.

4. Confinement with Chiral Symmetry

Our model for the relativistic description of heavy quark systems was defined in Sec. 2. The treatment of light quark systems, in particular the pion, requires the construction of an interaction consistent with chiral symmetry. The general framework for the construction of such an interaction was outlined in Sec. 3. The task of this section is to work out the details of how such an interaction is imbedded in the relativistic formalism introduced in Sec. 2, and in this way define a relativistic model for the treatment of light quark systems which is consistent with chiral symmetry.

4.1 Quark self energy

The first step is to cast the self energy relations, (3.14), into a form consistent with the relativistic equation introduced in Sec. 2, in which one of the quarks is restricted to its

mass-shell. In preparation for this, note that the self energy bubble, shown in Fig. 1, has singularities arising from the internal quark propagator and from the linear kernel, which contains the q^4 term and a "subtraction" which regularizes the strong singularities of the linear term at $q^2 = 0$. The detailed form of the subtraction term is not known for the case when *both* of the quarks are off-shell, but we know there must be such a term even in this case. The role if this term would be to soften the singularities at $q^2 = 0$.

If the quark self energy bubble is evaluated by integrating first over the energy component q_0 , and if the singularities at $q^2 = 0$ are softened by the subtraction, we are lead naturally to the idea that the integral can be approximated by retaining only the contribution from the positive energy quark pole at

$$k^2 [1 - \Sigma^v(k^2)]^2 = [m_0 + \Sigma^s(k^2)]^2 \quad (4.1)$$

Assuming the dependence of Σ^v and Σ^s on k^2 is very weak, so that their derivatives with respect to k^2 can be neglected, this approximation gives the following result for the quark self energy relations, (3.14)

$$\begin{aligned} \Sigma^s(p^2) &= -2 \int \frac{d^3 k}{(2\pi)^3} \left(\frac{1}{2E_k} \right) V_{eff}(p-k) \left[\frac{m_0 + \Sigma^s}{(1 - \Sigma^v)^2} \right] \\ p^2 \Sigma^v(p^2) &= 2 \int \frac{d^3 k}{(2\pi)^3} \left(\frac{1}{2E_k} \right) V_{eff}(p-k) p_0 E_k \left[\frac{1}{1 - \Sigma^v} \right] \end{aligned} \quad (4.2)$$

where the second relation has been evaluated in the rest frame of the quark, and $\Sigma^s = \Sigma^s(m^2)$ and $\Sigma^v = \Sigma^v(m^2)$. Specializing to the case when the external quark is also on-shell, and renormalizing the potential strengths by $\sigma/(1-\Sigma^v)^2 \rightarrow \sigma$ and the masses by $m/(1-\Sigma^v) \rightarrow m$, gives the following two relations for m and $a = \Sigma^v/(1-\Sigma^v)$

$$\frac{m - m_0}{m} = - \int \frac{d^3 k}{(2\pi)^3} \left(\frac{1}{E_k} \right) V_{eff}(p - k) \quad (a)$$

$$m a = \int \frac{d^3 k}{(2\pi)^3} V_{eff}(p - k) \quad (b)$$

(4.3)

Since both the external and internal quarks are on-shell in the relations (4.3), we may substitute the form of V_{eff} given in Eq. (2.21). Note that, because of the constraint (2.20), the linear term *makes no contribution to the dynamical mass shift*, and Eq. (4.3a) relates this shift to the constant C

$$C = - \left(1 - \frac{m_0}{m} \right) \quad (4.4)$$

As the bare quark mass approaches zero, C should approach the critical value of -1 . However, in Sec. 2 we saw that the mass of the composite system approached zero when C approached -2 , not -1 . The reason for this discrepancy is that the bound state equation does not yet include all of the contributions essential to a complete description of bound states with masses $\mu \rightarrow 0$. The additional contributions which are necessary will be derived and discussed in subsection 4.2.

Before turning to this discussion, we offer a few additional remarks and comments about the Eqs. (4.3). (i) Note that both the linear and constant terms contribute to the equation for the renormalization constant a . It can be readily seen that the contribution from the linear term is positive, and therefore a is bounded from below by the contribution of the constant term. This in turn permits us to prove that the renormalization factor must be positive

$$\frac{1}{1 - \Sigma^v} = 1 + a \geq 1 + C = \frac{m_0}{m} \geq 0 \quad (4.5)$$

showing that, in the approximation leading to (4.4), the mass renormalization does not change the sign of the quark masses. (ii) To treat the dependence of functions Σ^v and Σ^v

on k^2 self consistently, it is sufficient to expand them to first order in $(k^2 - m^2)$. These additional derivative terms modify our results by as much as 50%, and deserve further study. (iii) It may seem unphysical to treat bound quarks, which cannot exist in isolation, by restricting them to their mass-shell. As we mentioned in the Introduction, in our model the quarks only appear to propagate freely when they are in the vicinity of other quarks, and it is the linear potential interaction *between neighboring quarks* which provides the confinement; the self energy of the confined quarks is finite.

We turn now to the issue of how to reconcile the relativistic equation with the chiral constraint (4.4).

4.2 Equations for almost massless bound states

As mentioned above, Eq. (2.23) is not a suitable starting point for the description of the pion because, as the current quark mass $m_0 \rightarrow 0$ and (therefore) $C \rightarrow -1$, it does not automatically produce a solution for a bound state with zero mass. Instead, zero mass bound states occur only when $C \rightarrow -2$. In this section we will show that this inconsistency arises because a second channel, or component, of the relativistic wave function has been omitted from (2.23). This component turns out to be negligibly small *except in cases where the bound state mass is very close to zero*, or when the quarks are very light. In such cases the problem is very relativistic, and the additional component cannot be neglected.

To see how this additional component arises, examine the singularities of the propagators for the two off-shell quarks, which occur in the equation (3.14). Ignoring the self energy factor Σ (or, alternatively, approximating it by a constant in the vicinity of the poles and renormalizing), there are four poles in the complex k_0 plane, shown in Fig. 3. These are at

$$\begin{aligned}
 k_0 &= E_k - \frac{1}{2}\mu - i\epsilon & 1a \\
 &= -E_k - \frac{1}{2}\mu + i\epsilon & 1b \\
 k_0 &= E_k + \frac{1}{2}\mu - i\epsilon & 2a \\
 &= -E_k + \frac{1}{2}\mu + i\epsilon & 2b
 \end{aligned} \tag{4.6}$$

where the poles of the quark and antiquark are labeled 1 and 2 respectively, and positive energy poles (for the direction of momenta shown in Fig. 2) are designated by the letter a ; negative energy ones by b . The positive energy poles lie in the lower half plane and negative energy ones in the upper half plane.

Equation (2.23) can now be obtained from Eq. (3.15) by doing the integration over k_0 and *retaining the pole 1a only*. This procedure can be justified in two different ways. First, it can be viewed as an approximation to Eq. (3.15) justified by the facts that (i) the singularities coming from the linear potential are "softened" by imposition of the constraint (2.20), the same argument used to justify the reduction of the quark self energy, and (ii) the pole (1a) gives the dominant contribution from quark propagator poles (in the loosely bound case shown in Fig. 3a where μ is close to $2m$). [The singularities coming from the wave function are also assumed to give smaller contributions.] Alternatively, in the context of relativistic meson theories,²⁴ where light mesons are exchanged between two heavy bosons, examination of the infinite sum of all *ladder and crossed ladder* exchange diagrams shows that, in the *limit where the heavy mass is infinitely larger than the exchanged mass*, this ladder sum is given *exactly* by the solution of the relativistic equation in which one of the heavy bosons is restricted to its mass shell, *i.e.* Eq. (2.23). The latter justification is clearly more convincing, but it also is not clearly relevant to the system under current study. In any case, the use of Eq. (2.23) can be justified on fairly general grounds.

Review of the above discussion shows why the method fails for bound states of nearly zero mass, and how to correct it. We see that as $\mu \rightarrow 0$, the two poles (1a) and (2a) approach each other, and *coincide* when $\mu = 0$ (see Fig. 3b). Clearly in this case we cannot neglect the pole at (2a) in favor of the one at (1a)! Furthermore, the residues, R , of the two poles are roughly proportional to the inverse of their distances from pole (2b), and this ratio is

$$\frac{R_{2a}}{R_{1a}} = \frac{2E_k - \mu}{2E_k} \quad (4.7)$$

showing that pole (2b) is unimportant for loosely bound systems (where μ is close to

$2m$), but of equal importance when μ is small. The correct equation for bound states with nearly zero mass must therefore include the contributions from pole (2a), which results in the introduction of another component of the wave function (with the antiquark on-shell) and two coupled equations for these two components.

The new coupled equations have the following general structure:

$$\begin{aligned}\Gamma_1(p, P) &= - \int \frac{d^3 k}{(2\pi)^3} \left\{ V_{11}(p, k; P) \frac{\Gamma_1(k, P)}{(2E_k - \mu)} + V_{12}(p, k; P) \frac{\Gamma_2(k, P)}{(2E_k + \mu)} \right\} \\ \Gamma_2(p, P) &= - \int \frac{d^3 k}{(2\pi)^3} \left\{ V_{21}(p, k; P) \frac{\Gamma_1(k, P)}{(2E_k - \mu)} + V_{22}(p, k; P) \frac{\Gamma_2(k, P)}{(2E_k + \mu)} \right\}\end{aligned}\quad (4.8)$$

where Γ_1 and Γ_2 are the two components of the vertex function, as illustrated in Fig. 4a, and the four V 's are the components of a matrix interaction kernel (Fig. 4b). The subscripts 1 and 2 now designate how the relative energy k_0 is fixed, with (1) the quark, (2) the antiquark, on-shell, according to the relations (1a) or (2a) of Eq. (4.6). The energy denominators appropriate to each channel were obtained as in the derivation of Eq. (2.19).

The energy transfer is different for each of the V 's, and this the key to their definitions. From Fig. 4b, one readily sees

$$\begin{aligned}q^2 &= (E_p - E_k)^2 - (\mathbf{p} - \mathbf{k})^2 && \text{(for } V_{11} \text{ and } V_{22} \text{)} \\ q^2 &= (E_p - E_k - \mu)^2 - (\mathbf{p} - \mathbf{k})^2 && \text{(for } V_{12} \text{)} \\ q^2 &= (E_p + \mu - E_k)^2 - (\mathbf{p} - \mathbf{k})^2 && \text{(for } V_{21} \text{)}\end{aligned}\quad (4.9)$$

In completing the definition of V_{eff} for each element of the potential matrix, we continue to impose the constraint (2.20), building up the kernel from three contributions: (i) the "leading" q^{-4} term defined in Eq. (2.22), with the appropriate q^2 taken from (4.9), (ii) an appropriate δ function subtraction with support in the region where V_{ij} is singular, designed to insure the constraint (2.20) and regularize the strong singularities in V , and

(iii) a "constant" potential of the same form used in Eq. (2.21). These principles require that $V_{11} = V_{22} = V_{eff}$, as defined in Eq. (2.21). The definitions of the off-diagonal potentials requires further discussion.

The first step in the definition of V_{12} and V_{21} is straightforward and unique. Our leading q^{-4} terms, as defined above, are denoted by V_{RA}^{12} and V_{RA}^{21} . To implement the second step we must first decide how to impose the constraint (2.20). Consider $V_{21}(p, k)$ first. Because it is *not symmetric* in p and k , it will not be possible to require that (2.20) hold for both the initial and final channel *at the same time*. Stated another way, the imposition of the constraint on the incoming channel 1 will mean that *another* constraint (in which the RHS of (2.20) is not zero, but a finite function) will hold for the outgoing channel 2. We will chose to impose (2.20) on the *incoming* channel 1 for V_{21} and, as required by hermiticity, impose it on the *outgoing* channel (also 1) for V_{12} . Next, the second step requires that we find the region where $q^2 = 0$. This involves a surprising amount of analysis, and is described in the Appendix. The singularities of V_{RA}^{12} and V_{RA}^{21} can be easily characterized using a cylindrical coordinate system oriented in the direction of \mathbf{p} , with components k_{\perp} and k_{\parallel} . In this coordinate system, the singularities lie on conics of revolution, bounded either by points where $k_{\perp} = 0$, or where both k_{\perp} and $k_{\parallel} \rightarrow \infty$. When $k_{\perp} = 0$, k_{\parallel} may be either positive or negative, corresponding to \mathbf{k} either parallel or antiparallel to \mathbf{p} . For a given magnitude of p and bound state mass μ , there is, therefore, a range of values of the magnitude of k over which V is singular. We will denote the lower and upper limits of this region by k_1 and k_2 , respectively. The values of k_1 and k_2 for different regions of p and μ are given below and in the Appendix.

Now that the locations of the singularities of V_{RA}^{12} and V_{RA}^{21} are known, we must decide how to carry out the subtraction (in channel 1) which will remove them from the effective potential. In cases where the wave function depends only on the magnitude of k , which is the case here, we will remove, or "cut out", the entire region between k_1 and k_2 , and perform an additional subtraction at the *boundary* of the region. The removal of the entire *interior* of the singular region is justified by the observation that the precise location of the singularity inside the region depends on *both* k_{\perp} and k_{\parallel} , and hence any subtraction which depends only on the magnitude of k will cancel completely. For V_{21} , the final result of these considerations gives the following:

$$V_{21}(p, k; P) = \begin{cases} V_{RA}^{21}(p, k) - E_k \delta(\xi(p) k_1 \hat{\mathbf{p}} - \mathbf{k}) \int_{k' < k_1} \frac{d^3 k'}{E_{k'}} V_{RA}^{21}(p, k') & \text{if } k < k_1 \\ 0 & \text{if } k_1 < k < k_2 \\ V_{RA}^{21}(p, k) - E_k \delta(k_2 \hat{\mathbf{p}} - \mathbf{k}) \int_{k' > k_2} \frac{d^3 k'}{E_{k'}} V_{RA}^{21}(p, k') & \text{if } k_2 < k \end{cases} \quad (4.10)$$

where

$$k_1 = \left| p - \frac{\mu (2E_p + \mu)}{2(E_p - p + \mu)} \right|, \quad k_2 = p + \frac{\mu (2E_p + \mu)}{2(E_p + p + \mu)} \quad (4.11)$$

and

$$\xi(p) = \begin{cases} 1 & \text{if } \mu < m, \text{ and } p > \frac{\mu}{2} \left[1 + \frac{m}{m - \mu} \right] \\ -1 & \text{otherwise} \end{cases} \quad (4.12)$$

(see the Appendix for details). Note that the definition (4.10) insures that any integrals over V_{21} are finite by completely removing the *interior* of the region where V_{RA}^{21} is singular and by subtracting terms which regularize V_{RA}^{21} at the *boundary* of the region of singularities. Note also that our definition insures that V_{21} will equal the linear terms in V_{eff} [the first two terms in (2.21)] when $\mu = 0$.

The other potential V_{12} can now be obtained in one of two equivalent ways. First, we may use hermiticity to conclude that

$$V_{12}(p, k; P) = V_{21}(k, p; P) \quad (4.13)$$

Alternatively, it should be possible to find a form similar to (4.10), but with the appropriate q^2 taken from Eq. (4.9), k_1 and k_2 modified as described in the Appendix, and (new) subtraction terms consistent with the (new) constraint which holds for channel 2, as discussed above. Such a form would be convenient because it would express the subtraction directly in terms of the integration variable k , but in this paper we will rely on

(4.13).

So far, the definitions of the off-diagonal potentials have been a relatively straightforward generalization of the philosophy initially developed in Sec. 2. The last step in their construction is the choice of a "constant" term, similar to the last term in Eq. (2.21). So far we have not found a unique way of constructing this term. We know that chiral symmetry requires that the diagonal and off-diagonal potentials be equal when $\mu = 0$, and in this paper we chose the constant terms to be equal for all μ , the simplest choice consistent with this requirement. With this choice the coupled equations (4.8) become

$$\begin{aligned}
(2E_p - \mu + E_p C) \Psi_1(p) + E_p C \Psi_2(p) &= - \int \frac{d^3 k}{(2\pi)^3} V_{RA}(p, k) \left[\Psi_1(k) - \left(\frac{E_p}{E_k} \right) \Psi_1(p) \right] \\
&\quad - \int \frac{d^3 k}{(2\pi)^3} V_{12}(p, k) \Psi_2(k) \\
(2E_p + \mu + E_p C) \Psi_2(p) + E_p C \Psi_1(p) &= - \int \frac{d^3 k}{(2\pi)^3} V_{RA}(p, k) \left[\Psi_2(k) - \left(\frac{E_p}{E_k} \right) \Psi_2(p) \right] \\
&\quad - \int_{k < k_1} \frac{d^3 k}{(2\pi)^3} V_{RA}^{21}(p, k) \left[\Psi_1(k) - \left(\frac{E_k}{E_k} \right) \Psi_1(k_1) \right] \\
&\quad - \int_{k > k_2} \frac{d^3 k}{(2\pi)^3} V_{RA}^{21}(p, k) \left[\Psi_1(k) - \left(\frac{E_{k_2}}{E_k} \right) \Psi_1(k_2) \right]
\end{aligned} \tag{4.14}$$

where the explicit form for V_{12} remains to be worked out, and the coupled wave functions are

$$\Psi_1(p) = \frac{\Gamma_1(p, P)}{(2E_p - \mu)} \quad \Psi_2(p) = \frac{\Gamma_2(p, P)}{(2E_p + \mu)} \tag{4.15}$$

The extension of our model to deeply bound states is now complete. Note that if the extra channel described by Ψ_2 is neglected, the equations (4.14) become identical to the one channel equation (2.23), and that if $\mu = 0$, the equations have the solution

$$\Psi_1(p) = \Psi_2(p) = \frac{N}{E_p} \quad (4.16)$$

provided $C = -1$, as required by chiral symmetry. The equations (4.14) reconcile the requirements of relativity with chiral symmetry

As in the one channel case discussed in Sec. 2, we can use the uncertainty relation to estimate the behavior of the solutions to (4.14). For the heavy quark case studied in Sec. 2, the linear parts of the off diagonal potentials are much smaller than the linear parts of the diagonal potentials (see Figs 5 and 6 in Sec. 5) for all but the smallest bound state masses, so we will neglect them. We will also assume that the wave functions Ψ_1 and Ψ_2 have the same shape, with different normalizations, f_1 and f_2 , respectively (this is also true of the exact solutions). Then the coupled equations for the expectation values become

$$\begin{aligned} (p_o^2 [1 + \tfrac{1}{2}C] + 2 + C - \mu_o) f_1 + (1 + \tfrac{1}{2}p_o^2) C f_2 &= -\sigma_o r_o f_1 \\ (1 + \tfrac{1}{2}p_o^2) C f_1 + (p_o^2 [1 + \tfrac{1}{2}C] + 2 + C + \mu_o) f_2 &= -\sigma_o r_o f_2 \end{aligned} \quad (4.17)$$

where the energy has been expanded as in the derivation of Eq. (2.26). Solving these equations for μ_o , minimizing, and then calculating f_2/f_1 , gives the following estimates

$$r_o \approx \left(\frac{1+C}{\sigma_o [2+C]} \right)^{\frac{1}{3}}, \quad \mu_o^2 = 4(1+C) + 6(\sigma_o^2 (2+C)^2 [1+C])^{\frac{1}{3}}, \quad \frac{f_2}{f_1} = \frac{2m - \mu}{2m + \mu} \quad (4.18)$$

Note that both the size and mass of the bound state approach zero as $C \rightarrow -1$, and that the strength of the extra channel grows as $\mu \rightarrow 0$, becoming equal to the larger channel when $\mu = 0$. All of these results are well reproduced by the exact solutions, as discussed in the next section. Finally, using Eq. (4.4), the bare quark mass may be expressed in terms of f_1 and f_2 , and the dynamical mass m :

$$m_o = \left(\frac{f_1 - f_2}{f_1 + f_2} \right)^2 m \quad (4.19)$$

This concludes our theoretical discussion of the equation (4.14). We now turn to a review of the numerical results.

5. Solutions

In this section we discuss our numerical techniques and present solutions to our bound state equations in two limits: (i) the heavy quark case, where $m^2 \gg \sigma$ and (ii) the light quark case where $m^2 \sim \sigma$.

5.1. Numerical Methods

In this first paper we choose to solve the coupled equations (4.14) for the constant C as a function of the bound state mass μ and with (at this point, arbitrarily) fixed parameters σ_o and Λ_o . We already know the solution to the equations in two extreme limits: 1) the true nonrelativistic limit where $\Psi_1(p)$ is simply the fourier transform of the first Airy function and $\Psi_2(p) \sim 0$, and 2) the zero mass pion case, $\mu=0$, where $\Psi_1(p)=\Psi_2(p)=1/E(p)$. These two limiting solutions behave very differently at large momenta p (the nonrelativistic solution having a rapid fall-off, whereas the zero mass pion case has a long tail) and the challenge is to develop a technique for solving the equations that can interpolate between these two limits. In addition, there is the technical problem of handling the poles in the integrands arising from the potentials V_{11} , V_{12} and V_{21} .

To solve the equations, we first expand each wavefunction, $\Psi_1(p)$ and $\Psi_2(p)$, in terms of a finite set of basis functions, $\{b_i(p)\}$, and then solve for the coefficients of this expansion, and for the value of the constant C . A principal reason for using analytic basis functions is that there are then no difficulties in performing the integrals over the singularities in the integrand. For each basis function $b_j(p)$, each term in equation (4.14) is first evaluated, and then expanded in terms of the set $\{b_i(p)\}$; for example, we expand the product $E(p)b_j(p)$. Since this product [or any of the other terms in Eq. (4.14)] is not in general exactly expressible as a linear combination of the finite set $\{b_i(p)\}$, a linear

least squares procedure is used to obtain the best fit possible. For a basis set with n functions, we thus construct (for given μ , σ_o and Λ_o) from Eq. (4.14) a generalized eigenvalue problem $A\mathbf{x}=\lambda B\mathbf{x}$, where A and B are matrices of dimension $(2n)\times(2n)$ containing the coefficients of the linear least squares expansion, the eigenvector \mathbf{x} is of length $(2n)$ whose entries (which we are solving for) are the expansion of the wavefunctions $\Psi_1(p)$ and $\Psi_2(p)$, and the eigenvalue λ is the constant C . We solve for λ and \mathbf{x} using standard techniques and identify the ground state as that solution with the least negative (i.e. closest to zero) eigenvalue. We then iterate the procedure, increasing the number of basis functions in the set $\{b_i(p)\}$ until the solution converges. For the set $\{b_i(p)\}$, we use

$$b_j(p)=N_j L_j\left(\frac{p}{m_\ell}\right) e^{-\frac{1}{2}\frac{p}{m_\ell}} \quad (5.1)$$

where L_j is the j th Laguerre polynomial, m_ℓ is an arbitrary mass parameter, and N_j is a normalization factor with dimensions of inverse mass. The advantages of this choice of basis functions are: 1) the b_j are orthogonal over the interval $0 \leq p \leq \infty$, and; 2) in the limit $n \rightarrow \infty$, the set $\{b_i(p)\}$ is complete (any analytic function is expandable in terms of them), and therefore the method must in principle ultimately converge to the correct solution, independent of m_ℓ . In practice though, to obtain convergence rapidly the choice of m_ℓ is crucial and at times problematic.

5.2 Results

The first application of our numerical technique has already been presented in Sec. 2 where we solved the nonrelativistic equation (2.8) and quite accurately reproduced the known analytic results (see Table 1). The fully coupled relativistic equation is a much more complicated problem. One relevant issue concerning these equations and already briefly mentioned in Sec. 4, is the structure and relative sizes of the diagonal and off-diagonal integrals in Eq. (4.14). Whereas one cannot unambiguously discuss this point for every m and μ without knowing the full solutions $\Psi_1(p)$ and $\Psi_2(p)$, a comparison of these

integrals over the first Laguerre basis function $b_1(p)$ should be indicative. In Figs. 5 and 6 the integrals of $b_1(p)$ over V_{11} and V_{21} [as they appear in Eq. (4.14)] are presented as a function of the dimensionless variable (p/m) for two different values of μ/m . [Recall V_{12} has been defined from V_{21} through hermiticity, Eq. (4.13).] We see that these curves are smooth and that the off-diagonal integrals are slowly developing into the V_{11} contribution as the bound state mass approaches zero. In fact it is only for the most deeply of bound systems that the off-diagonal elements V_{21} (and hence V_{12}) are at all appreciable. For simplicity we have thus accordingly set these terms to zero. These curves also depend on the Laguerre mass, m_L and the cutoff mass Λ_o . We took $\Lambda_o = 1.7$. Although our value is at this stage somewhat arbitrary, Λ_o has been chosen so that the integral over V_{11} traces fairly closely its corresponding non-relativistic version, V_L , in Eq. (2.5) and thus preserves the low energy, linear confining features of our potential. The integral over V_L has likewise also been included in these figures. The value of the Laguerre mass, $m_L = 0.17m$, is the same as the one used to obtain the solutions in both the heavy and light quark regimes. Although convergent solutions do not depend on m_L , gross errors in the choice of the Laguerre mass (such as a factor of ten) make such solutions unobtainable with only a few basis functions ($n \sim 10$).

a) the case of heavy quarks ($m^2 \gg \sigma$)

In this situation there are two scales to the problem and accurate, numerical solutions are subsequently relatively easy to obtain until the very smallest bound state masses. For σ we take a value consistent with lattice studies and nonrelativistic models: $\sigma = 0.2(\text{Gev})^2$. For the heavy quark case, we then taken $m=3.5$ Gev, approximately a factor of ten larger than what might be considered a reasonable value for the constituent mass of the up and down quarks. This value for m is also, coincidentally, approximately the mass of the bottom quark. It should be emphasized that in this section we are only obtaining test solutions to our equations and that no physical meson should yet be associated with any of these solutions. In particular, we're not claiming that a deeply bound pseudoscalar state of bottom quarks exists. We could have equally chosen to work in this section with a value of both σ and m ten times smaller.

For this case both the one and two channel equations [(2.23) and (4.14) respectively]

were solved for a variety of bound state masses. The results are shown in Figs. 7-10. Figure 7 plots the value of the constant C for both channels versus the bound state mass, μ . The circles are our numerical solutions. The smooth curves are the estimates made in Secs. 2 and 4 for the relation between μ and C , and given by equations (2.27) and (4.18), respectively. We see close agreement between our solutions and these estimates. Figure 8 plots the ratio of $\Psi_2(0)/\Psi_1(0)$ for the two channel solutions, and the estimate for this ratio given in equation (4.18). Again there is close agreement between the two, perhaps beyond what might be expected since these estimates involve a non-relativistic expansion of the energy factor $E(p)$ which is certainly incorrect in the limit $C \rightarrow -1.0$ (or -2.0 in the one channel case). However the success of these estimates probably relies more on the small size of σ_o (~ 0.02) and the ignorability of the off-diagonal integrals (as suggested in Figs. 5 and 6) than the average size of the momenta, p .

In Figs. 9 and 10 the wave functions for both the one and two channel solutions are plotted for two illustrative bound state masses. In the first case of small binding energy ($\mu = 6.0$), relativistic corrections are of the order of 10% as might be expected. More interesting is the fact that the wave function $\Psi_1(p)$ is unchanged in going from the one to two channel equation – the presence of the second channel being completely absorbed by a modification of the value of the constant C . For more tightly bound solutions (e.g., $\mu = 1.75$) this is no longer the case and $\Psi_1(p)$ is significantly modified, becoming broader in momenta space. In this case $\Psi_2(p)$ is also more significant. The necessity for using the fully coupled, relativistic equation in this limit is clear.

b) The case of light quarks ($m^2 \sim \sigma$)

Solutions have thus far been obtained in this case only for large bound state masses ($\mu \sim 2m$). For more deeply bound systems our numerical techniques have not so far given stable solutions. What is probably needed is a set of basis functions that individually more closely approximate the correct solutions, for even in the case of the lightly bound systems the convergence of the Laguerre series was slow, and we found great sensitivity in the value of the constant C and in the exact shape of the wavefunctions at large momentum (although the relative sizes of the two channels are much more stable). We thus defer a full analysis of the light quark case to a subsequent paper and only present here our results for

the lightly bound systems. These are still instructive.

We work with a quark mass $m=0.35$, while the coefficient of the linear potential $\sigma = 0.2$ as before. The solutions $\Psi_1(p)$ and $\Psi_2(p)$ for a bound state mass $\mu = 0.6$ are shown in Fig. 11. Note how much larger $\Psi_2(p)$ is here than in the analogous, $\mu = 6$ solution for the heavy quarks shown in Fig. 9. Preliminary results for more deeply bound systems ($\mu = 0.14$) strongly suggest this trend continues and that $\Psi_1(p)$ and $\Psi_2(p)$ rapidly approach equal value. As expected for the case of light quarks, even moderately bound systems are highly relativistic and use of the fully coupled, two-channel equation is absolutely necessary. No nonrelativistic (one-channel) reduction can be made.

The solution in Fig. 11 corresponds to a value of the constant $C \sim -1.3$. The fact that $C < -1.0$ is not yet understood in conjunction with our quark self-energy relation, equation (4.4), which would appear to suggest such a value is unphysical. The source of this discrepancy may be due to one or more of the following factors: (i) the approximations made concerning the quark propagator in deriving the bound state equations (4.14), namely, the simplification of replacing the full quark propagator by a Feynman propagator with a constant mass, (ii) ambiguities in defining the off-diagonal constant potential, (iii) the neglect of the off-diagonal elements V_{21} and V_{12} , or (iv) inaccuracies in our numerical method for the determination of C , which may be as large as 20% in the light quark case. Although an intriguing issue, especially considering the nice results obtained for C vs. μ in the heavy quark case presented in Fig. 7, we feel that further discussion of the constant C must be postponed until a full systematic study of the light quark case has been successfully completed.

6 Conclusions

A new model of mesons has been introduced that is covariant, confining and which includes chiral symmetry. In this fashion we are developing a unified description of all the mesons, from the pion to the upsilon. The exact definition of our approach awaits later work when the small number of parameters in our model are determined by fitting the full meson spectrum. Our equations are analytically solvable in the limit of absolute chiral

symmetry (i.e., zero pion mass) and reproduce the very successful nonrelativistic linear potential models in the case of lightly bound, heavy quark systems.

We have obtained numerical solutions for a pseudoscalar bound state in the case of heavy quarks and arbitrary bound state mass. Further work along these lines remains for the case of light quarks. One important ingredient that needs to be added is the effect of one gluon exchange. As OGE effects are expected to be especially large in the case of light quarks, their inclusion will be an important part in the next stage of development.

Acknowledgements

We are grateful for the support of the Department of Energy under grant no. DE-FG05-88ER40435. We thank M. K. Banerjee and T. D. Cohen for a very useful conversation, and also wish to thank the physicists and staff at the INFN, Sezione Sanita, in Rome, and at the Institute for Theoretical Physics, University of Utrecht, for hospitality during visits when some of this work was done.

Appendix

In this appendix we will determine the location of the singularities of V_{RA}^{21} and V_{RA}^{12} . These occur when $q^2 = 0$. Introducing components of k parallel to and perpendicular to p , and defining $k_{||}' = k_{||} - p$, the location of the singularities can be determined from Eq. (4.9), which becomes

$$(E_p - E_k \pm \mu)^2 = (k_{||}')^2 + k_{\perp}^2 \quad (\text{A.1})$$

where in Eq. (A.1) and all subsequent equations the upper sign refers to V_{RA}^{21} and the lower one to V_{RA}^{12} . Expanding the square on the LHS gives

$$(E_p \pm \mu)^2 + E_p^2 + 2p k_{||}' = 2E_k(E_p \pm \mu) \quad (\text{A.2})$$

If both sides of this equation have the same sign, it may be squared without introducing spurious roots. Since the RHS is always positive for V_{RA}^{21} , this reduces to the following restriction on $k_{||}'$ if it is to be a root of (A.2)

$$(E_p + \mu)^2 + E_p^2 + 2p k_{||}' > 0 \quad (\text{A.3})$$

For V_{RA}^{12} , there are two cases depending on whether or not E_p is bigger or less than μ :

$$(E_p - \mu)^2 + E_p^2 + 2p k_{||}' > 0 \quad (\text{a})$$

$$(E_p - \mu)^2 + E_p^2 + 2p k_{||}' < 0 \quad (\text{b}) \quad (\text{A.4})$$

If E_p is greater than μ , the roots must satisfy condition (A.4a), while if E_p is less than μ they must satisfy (A.4b). Keeping this in mind, (A.2) can be squared and written in the following form:

$$\alpha k_{\perp}^2 + \beta (k_{\parallel} - k_a)(k_{\parallel} - k_b) = 0 \quad (\text{A.5})$$

where

$$\begin{aligned} \alpha &= 4(E_p \pm \mu)^2 & \beta &= \alpha - 4p^2 = 4[E_p \pm \mu + p][E_p \pm \mu - p] \\ k_a &= p \pm \frac{\mu(2E_p \pm \mu)}{2(E_p + p \pm \mu)} & k_b &= p \mp \frac{\mu(2E_p \pm \mu)}{2(E_p - p \pm \mu)} \end{aligned} \quad (\text{A.6})$$

Equation (A.5) shows that the singularities lie on conic sections of revolution, which are ellipsoids if $\beta > 0$ and hyperboloids if $\beta < 0$.

Consider the potential V_{RA}^{21} first. In this case β is always positive, and the singularities lie on an ellipsoid of revolution bounded between k_b (which can be negative) and k_a (which is always positive and larger than k_b). Furthermore, k_a is never so negative that it violates the condition (A.3). Expressed in terms of the magnitude of k , we see that the singularities are first encountered when $k = |k_b|$, and that when $k > k_a$ there are also again no more singularities. Cutting out the region where the location of singularities depends on *both* k_{\perp} and k_{\parallel} gives the results recorded in Table 2, with $k_1 = |k_b|$ and $k_2 = k_a$. Finally, $k_a < 0$ means that \mathbf{k} is antiparallel to \mathbf{p} , requiring the ξ defined in Eq. (4.12) to be -1 , and the range of p over which this occurs is as given in Eq. (4.12). The boundaries of the singular region are shown in Fig. 12a and c.

The direct analysis of V_{RA}^{12} is considerably more complicated because β can be negative. As p is increased from zero, β is first positive, but then changes sign when p reaches the critical point

$$p_{crit} = \frac{|m^2 - \mu^2|}{2\mu} \quad (\text{A.7})$$

If $\mu < m$, this happens because $E_p - p + \mu$ goes through zero at this point, causing $k_b \rightarrow +\infty$ (when $p < p_{crit}$) and then (when $p > p_{crit}$) increase from $-\infty$. The large negative value of k_b is associated with the second branch of the hyperboloid of revolution, which need not be considered, however, because this root is spurious, violating the

inequality (A.4a). Hence the only singularities of V_{RA}^{12} , for $\mu < m$, lie between $k_1 = |k_a|$ and $k_2 = k_b$ (if $p < p_{crit}$), or $k_2 = \infty$ (if $p > p_{crit}$), consistent with Table 2. Next, if $\mu > m$, the critical point is reached when $E_p + p - \mu = 0$, because the other factor in β , $E_p - p - \mu$, is always negative. But when $p < p_{crit}$ it turns out that *neither* k_a *nor* k_b satisfy the inequalities (A.4), showing that they are both spurious roots, and that V_{RA}^{12} has *no* singularities when $p < p_{crit}$. In the language of Table 2 and Eq. (4.10) this means that $k_1 = k_2 = \infty$. Finally, when $p > p_{crit}$, the root k_2 is spurious, and the singularities lie along only one branch of a hyperboloid of revolution, bounded by $k_1 = |k_a|$ and ∞ , as given in Table 2. In both cases, k_a is positive, and hence \mathbf{k} is parallel to \mathbf{p} , only if $p > \mu [1 + \mu/2(m + \mu)]$. The boundaries of the singular regions for V_{12} are shown in Fig. 12b and c. Note that these are related to those of V_{21} by $p \leftrightarrow k$, as required by hermiticity.

An explicit form for V_{12} , similar to that given for V_{21} in Eq. (4.10), can be obtained by using Eq. (4.13) and the definitions of k_1 and k_2 worked out above and summarized in Table 2, but, since we have neglected these terms in this work, this will be postponed to a subsequent paper.

References

1. C.E. Carlson and F. Gross, Phys. Rev. Lett. 53, 127 (1984).
2. A. Chodos, R. L. Jaffe, K. Johnson, C. B. Thorn and V. Weiskopf, Phys. Rev. D9, 3471 (1974); T. DeGrand, R. L. Jaffe, K. Johnson, and J. Kiskis, Phys. Rev. D12, 2060 (1975).
3. A. Chodos and C. B. Thorn, Phys. Rev. D12, 2733 (1975).
4. W. A. Bardeen, M. S. Chanowitz, S. D. Drell, M. Weinstein, and T. M. Yan, Phys. Rev. D11, 1094 (1975).
5. C. G. Callan, R. F. Dashen, and D. J. Gross, Phys. Rev. D19, 1826 (1979); V. Vento, M. Rho, E. Nyman, J. Jun and G. E. Brown, Nucl. Phys. A345, 413 (1980); F. Myhrer, G. E. Brown, and Z. Xu, Nucl. Phys. A362, 317 (1981).
6. G. E. Brown, A. S. Goldhaber, and M. Rho, Phys. Rev. Lett. 51, 747 (1983); J. Goldstone, and R. L. Jaffe, Phys. Rev. Lett. 51, 1518 (1983); I. Zahed, A. Wirzba, and U. G. Meissner, Ann. Phys. 165, 406 (1985).
7. S. Theberge, A. W. Thomas, and G. A. Miller, Phys. rev. D22, 2838 (1980); *ibid* D24, 216 (1981).
8. R. Goldflam and L. Wilets, Phys. Rev. D25, 1951 (1982).
9. R. Friedberg and T. D. Lee, Phys. Rev. D15, 1694 (1977); *ibid* 16, 1096 (1977); *ibid* 18, 2623 (1978).
10. H. B. Nielsen and A. Patkos, Nucl. Phys. B195, 137 (1982).
11. G. Chanfray, O. Nachtmann, and H. J. Pirner, Phys. Lett. 147B, 249 (1984).
12. W. Broniowski, T. D. Cohen, and M. K. Banerjee, Phys. Lett. B187, 229 (1986).
13. G. Fai, R. J. Perry, and L. Wilets, Phys. Lett. B208, 1 (1988).
14. F. Lenz, J. T. Londergan, E. J. Monitz, R. Rosenfelder, M. Stingl, and K. Yazaki, Ann. Phys. 170, 1 (1986).

15. S. Godfrey and N. Isgur, Phys. Rev. D32, 189 (1985).
16. A. DeRujula and F. Martin, Phys. Rev. D22, 1787 (1980); R. L. Jaffe and G. G. Ross, Phys. Lett. B93, 313 (1980); C. J. Benesh and G. A. Miller, Phys. Rev. D36, 1344 (1987); R. P. Bickerstaff and A. W. Thomas, J. Phys. G15, 1523 (1989).
17. V. Bernard, R. Brockmann, M. Schoden, W. Weisse, and E. Werner, Nucl. Phys. A412, 349 (1984); V. Bernard, R. Brockmann, and W. Weisse, Nucl. Phys. A440, 605 (1985).
18. A. LeYaouanc, L. Oliver, O. Pene, and J-C. Raynal, Phys. Rev. D29, 1233 (1984); A. LeYaouanc, L. Oliver, S. Ono, O. Pene, and J-C. Raynal, Phys. Rev D31, 137 (1985).
19. Pedro J. de A Bicudo and Jose E. F. T. Ribeiro, Phys. Rev. D42, 1611 (1990); *ibid*, 1625; *ibid*, 1635.
20. For review see J. B. Kogut, Rev. Mod. Phys. 51, 659 (1979); *ibid*, 55, 775 (1985).
21. Y. Nambu and G. Jona-Lasinio, Phys. Rev. 122, 345 (1964); *ibid*, 124, 246 (1961).
22. F. Gross, Phys. Rev. D10, 223 (1974); W. W. Buck, F. Gross, Phys. Rev. D20, 2361 (1979); F. Gross, J. W. Van Orden, K. Holinde, Phys. Rev. C41, 1909 (1990).
23. F. Gross, Invited talk presented to the European Workshop on Few Body Physics, Rome, Italy, published in the proceedings, Few Body Systems, Supp. 1, C. Ciofi degli Atti, O. Benhar, E. Pace, and G. Salme, eds., p. 433.
24. F. Gross, Phys. Rev. C26, 2203 (1982).
25. C. D. Roberts, R. T. Cahill, and J. Praschifka, Ann. Phys. 188, 20 (1988).
26. The Feynman Lectures on Physics, Vol.III,p.2-5, Feynman, Leighton, and Sands, Addison-Wesley, Reading, Mass. (1965).
27. V. Bernard, Phys. Rev. D34, 1601 (1986); T. Hatsuda and T. Kunihiro, Phys. Lett. B185, 304 (1987); V. Bernard, R. L. Jaffe, and U. G. Meissner, Nucl. Phys. B308, 753 (1988).

Table Captions:

1. Comparison of our numerical solutions to Eq. (2.8) with the exact analytic value given in Eq. (2.9). The mass of the quark was taken to be 0.35 GeV, that of the bound state 0.69 GeV, and the constant $C = 0$. We thus solved for $\lambda = 8\pi\sigma$.
2. The boundaries k_1 and k_2 of the region of singularities of the off-diagonal potentials V_{21} and V_{12} for different values of the momenta p and bound state mass μ .

Figure Captions

1. The self-consistent Dyson equation for the quark self-energy. Blobs represent the full quark propagator, while the heavy dashed line schematically represents the potential.
2. The equation for the vertex function.
3. The position of the poles, Eq. (4.6), in the quark propagators evaluated for $p=0$ and (a) $\mu \sim 2m$ and (b) $\mu \sim 0$.
4. The representation of the two vertex functions and four potentials. A quark line with an \times is on-shell.
5. The integrals of the first Laguerre basis function over the potentials V_{11} and V_{21} plotted versus the dimensionless variable p/m . The dashed line is the integral using the non-relativistic definition of the potential V_L , Eq. (2.5). The mass in our cutoff function $\Lambda_0=1.7$, the mass in the Laguerre basis function $m_L=0.17m$, and $\mu/m=0.5$. Note that V_{21} is all but ignorable.
6. The same as Fig. 5 except that now $\mu/m=0.125$.
7. Solutions for the constant C as a function of $\mu/2m$ for both the one and two-channel bound state equations in the case of heavy quark mass. Our numerical solutions are the large circles, while the curves are the estimates for the one and two-channel solutions given in Eq. (2.27) and (4.18) respectively.
8. The ratio $\Psi_2(0)/\Psi_1(0)$ as a function of μ/m . We use the same notation as in Fig. 7.
9. Our solutions for the wave functions for both the one and two-channel equations for the case of a lightly bound system of heavy quarks ($\mu/2m = 0.85$). The wavefunctions have been normalized such that $\Psi_1(0)=1$. The full and dashed curves are the two-channel solutions Ψ_1 and Ψ_2 , respectively, while the dotted curve is the one-channel solution. In this limit we see that a non-relativistic reduction is quite sensible.
10. The same as in Fig. 9 except now the quarks are deeply bound, $\mu/2m = 0.25$. The quarks are clearly now highly relativistic.

11. The solution for the wave functions of the two-channel equation in the case of a lightly bound system ($\mu/2m = 0.85$) of light quarks. As opposed to the analogous case of Fig. 9, no non-relativistic approximation is possible.

12. The heavy solid lines are the boundaries of the singular regions of the potentials V_{RA}^{12} and V_{RA}^{21} . (a) V_{RA}^{21} for $\mu < m$, (b) V_{RA}^{12} for $\mu < m$, (c) V_{RA}^{21} for $\mu > m$, and (d) V_{RA}^{12} for $\mu > m$. In each figure the vertical axis is k and the horizontal axis is p , and the shaded lines are asymptotes.

Table 1

# basis functions	λ_{num}	$(\lambda_{\text{num}} - \lambda_{\text{theor}}) \times (10)^4$
4	1.2505596	.0804613
6	1.1795415	.0094432
8	1.1723112	.0022129
10	1.1710102	.0009119
12	1.1701975	.0000992
14	1.1701639	.0000656

Table 2

	k_1	k_2
	$\left p - \frac{\mu (2E_p - \mu)}{2(E_p + p - \mu)} \right $	$p + \frac{\mu (2E_p - \mu)}{2(E_p - p - \mu)}$
V_{12}	∞	∞
	$\left p - \frac{\mu (2E_p - \mu)}{2(E_p + p - \mu)} \right $	∞
V_{21}	$\left p - \frac{\mu (2E_p + \mu)}{2(E_p - p + \mu)} \right $	$p + \frac{\mu (2E_p + \mu)}{2(E_p + p + \mu)}$

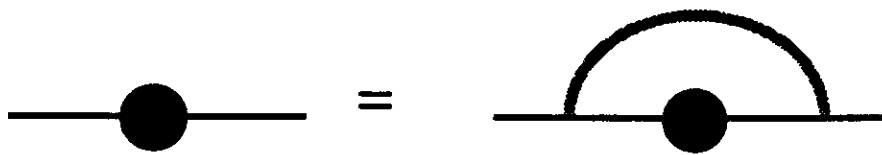


Fig. 1

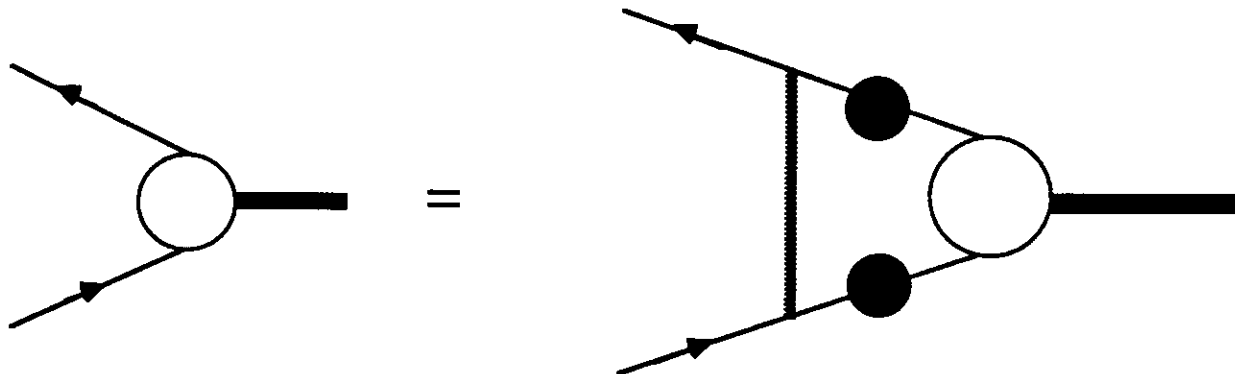
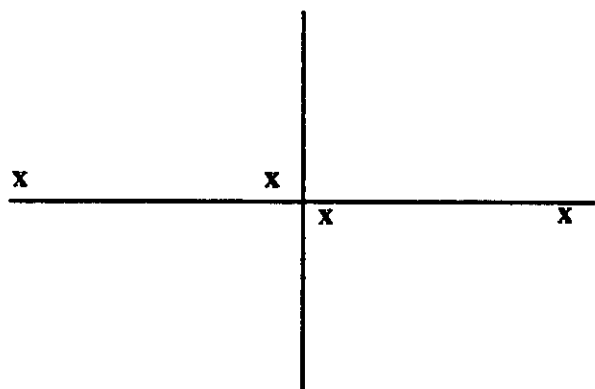
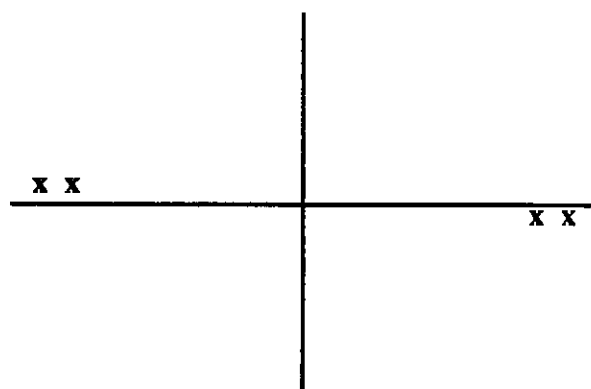


Fig. 2

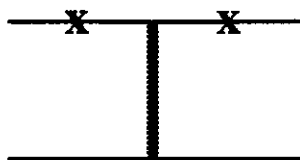
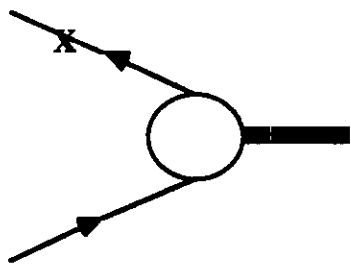


(a)

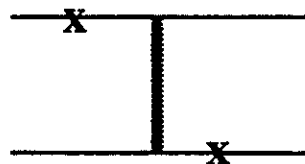


(b)

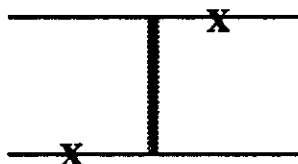
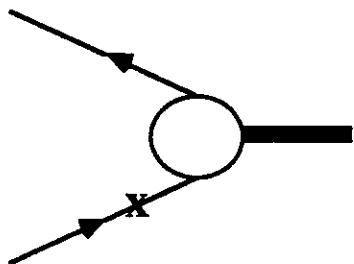
Fig. 3



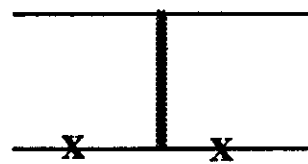
V_{11}



V_{12}



V_{21}



V_{22}

(a)

(b)

Fig. 4

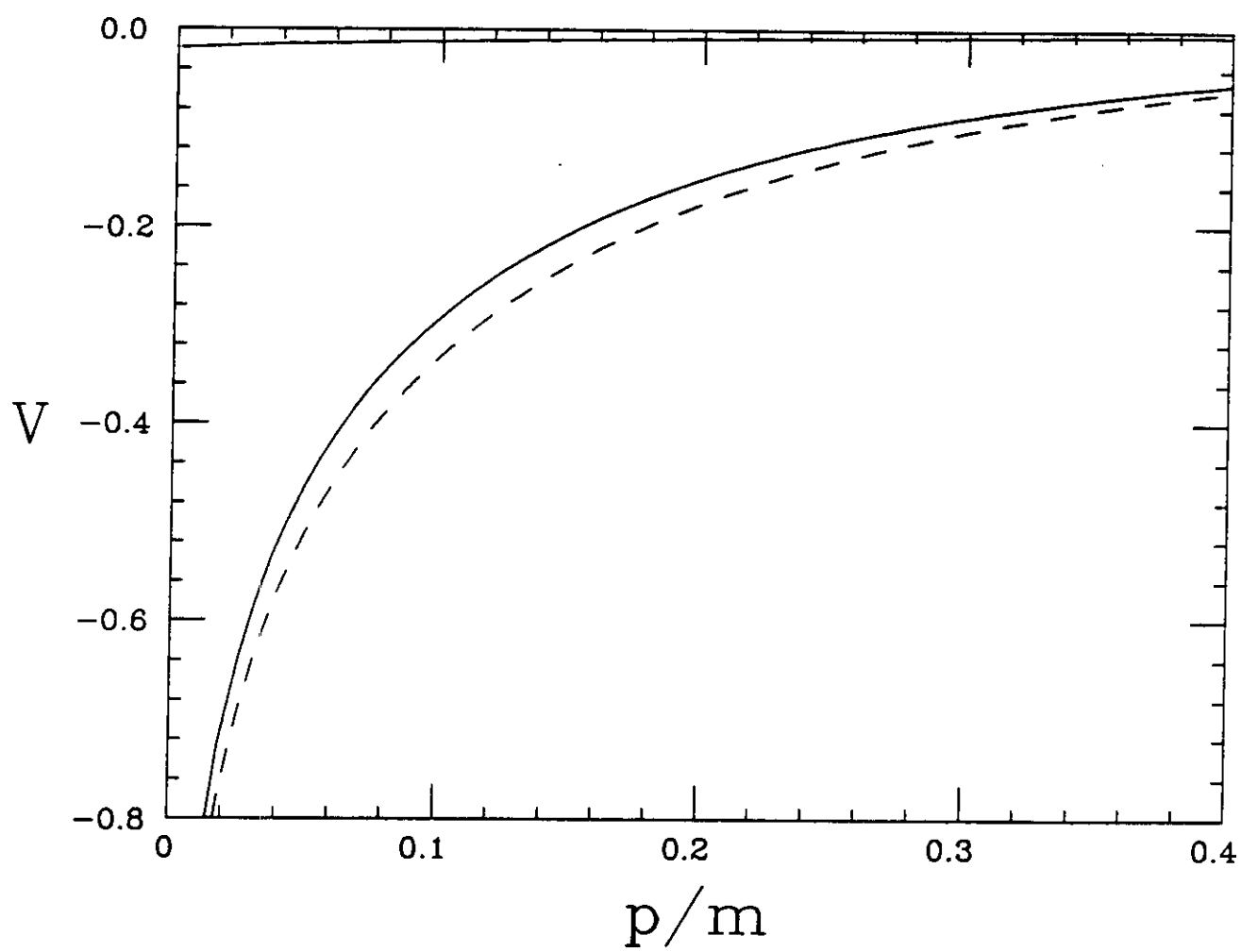


Fig. 5

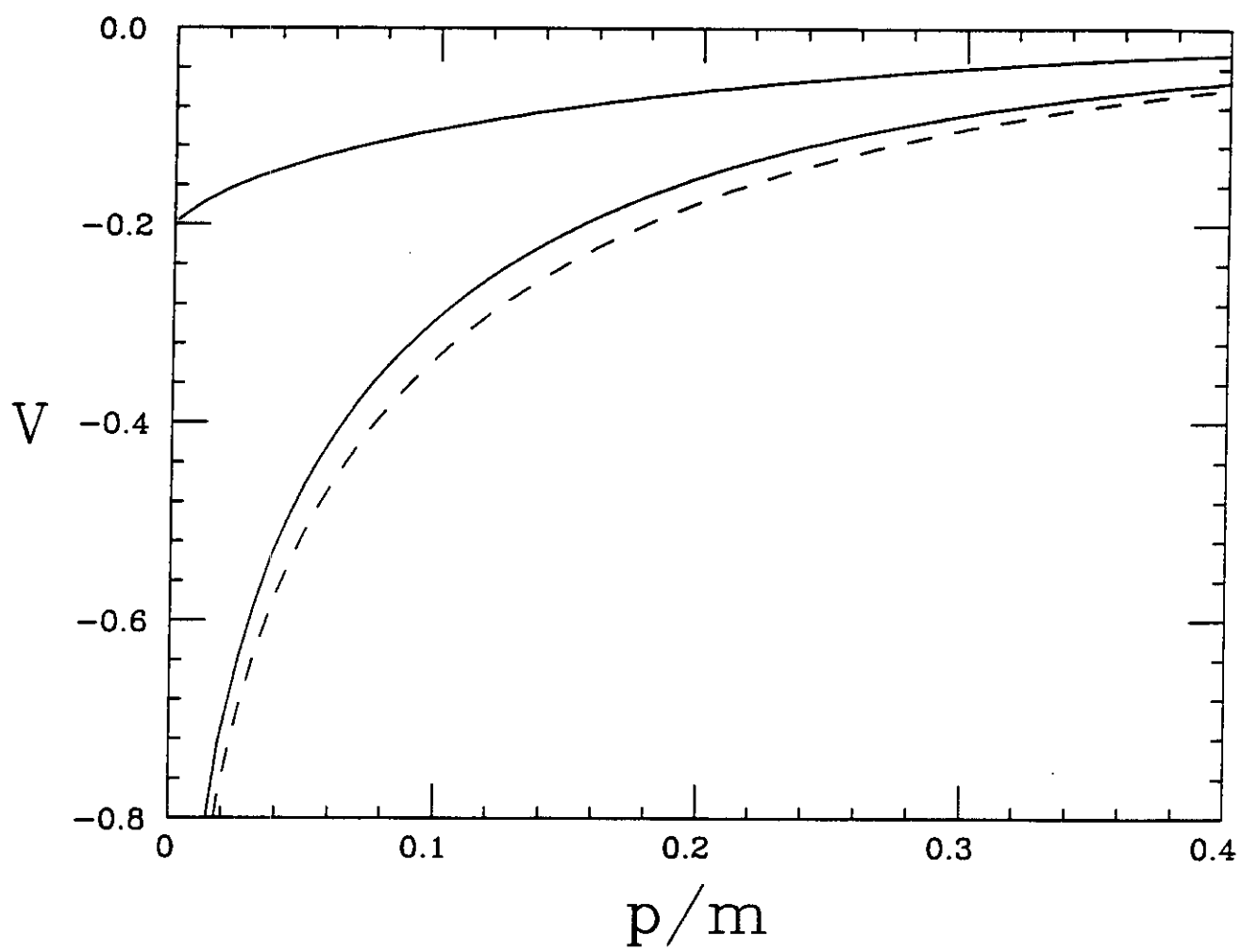
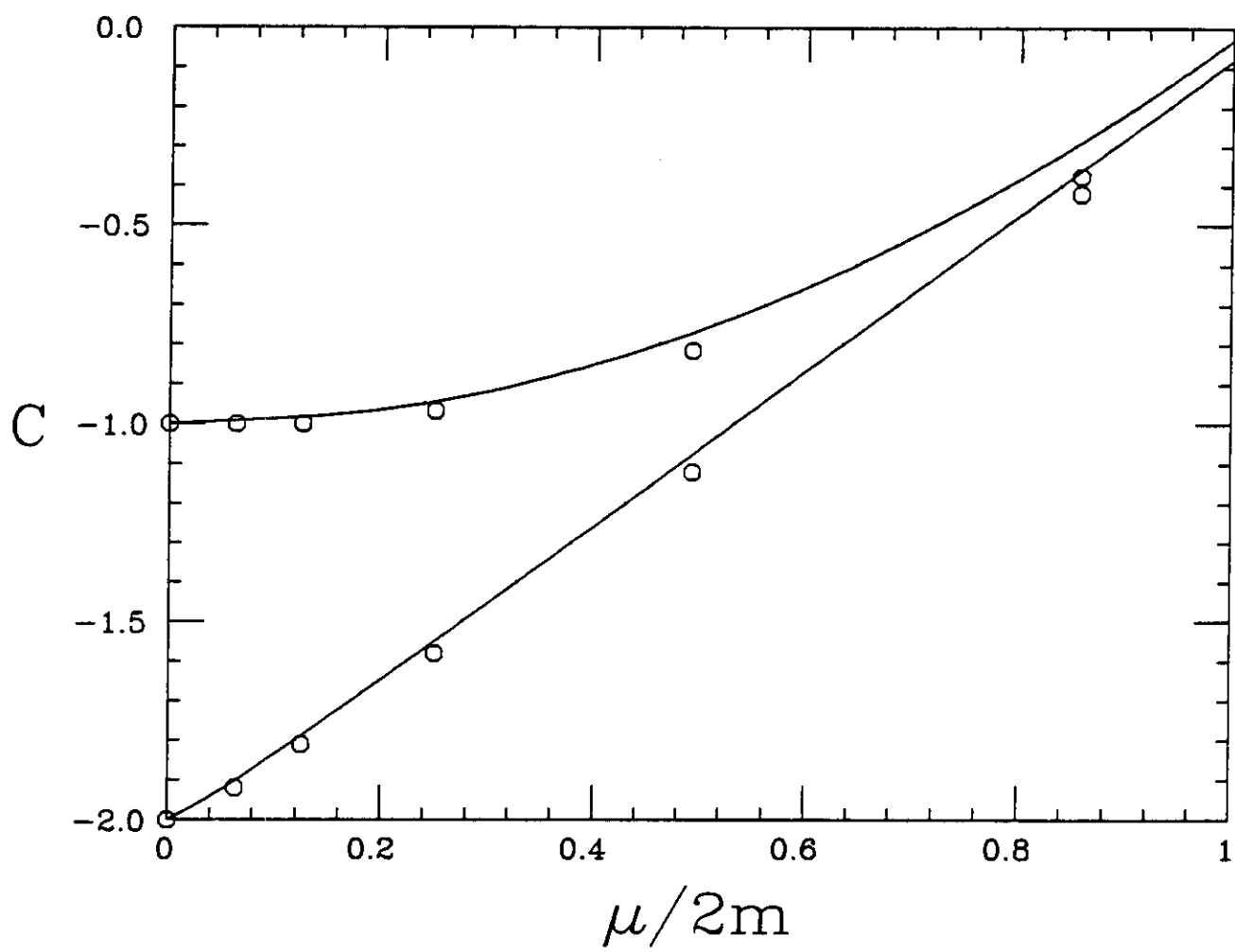
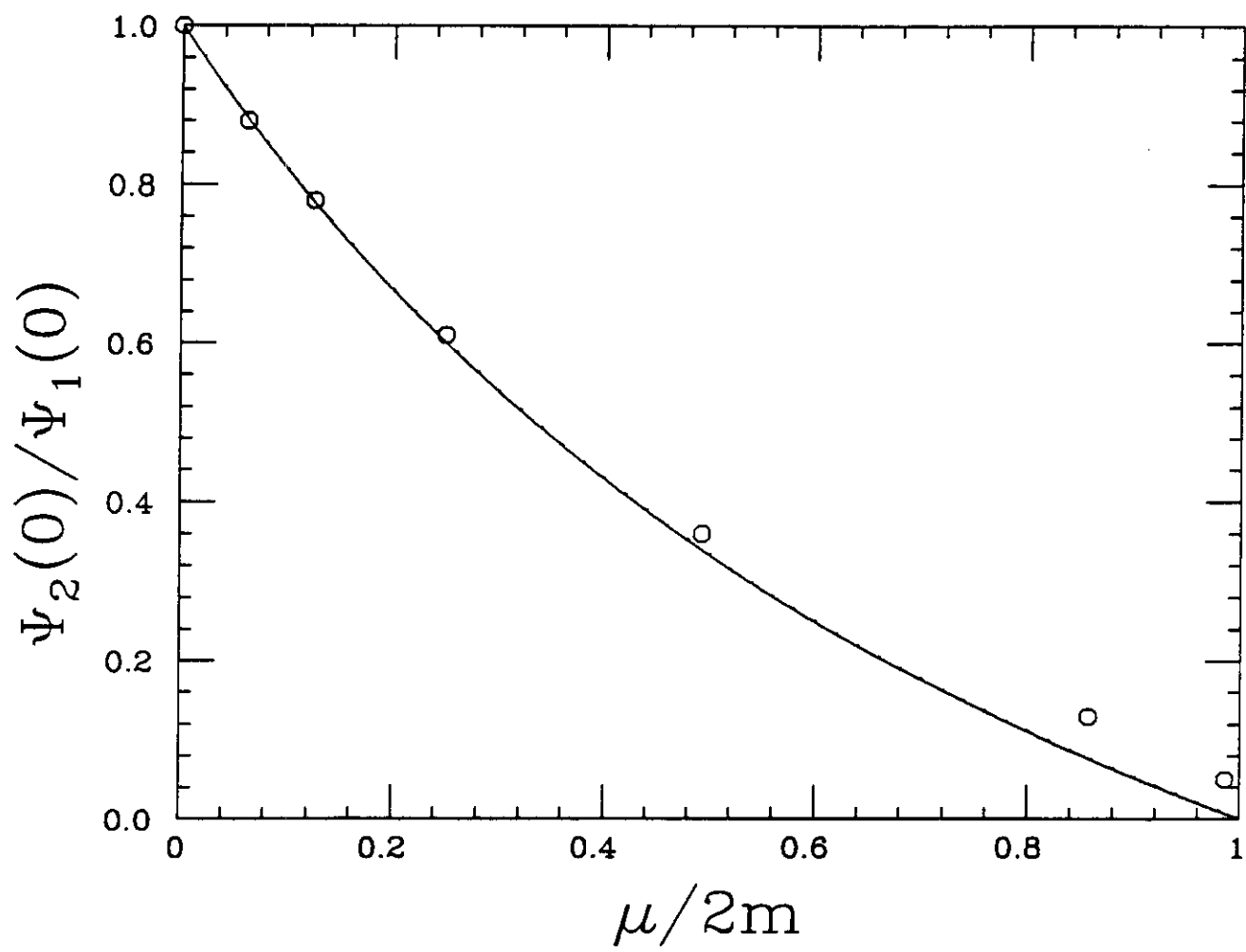
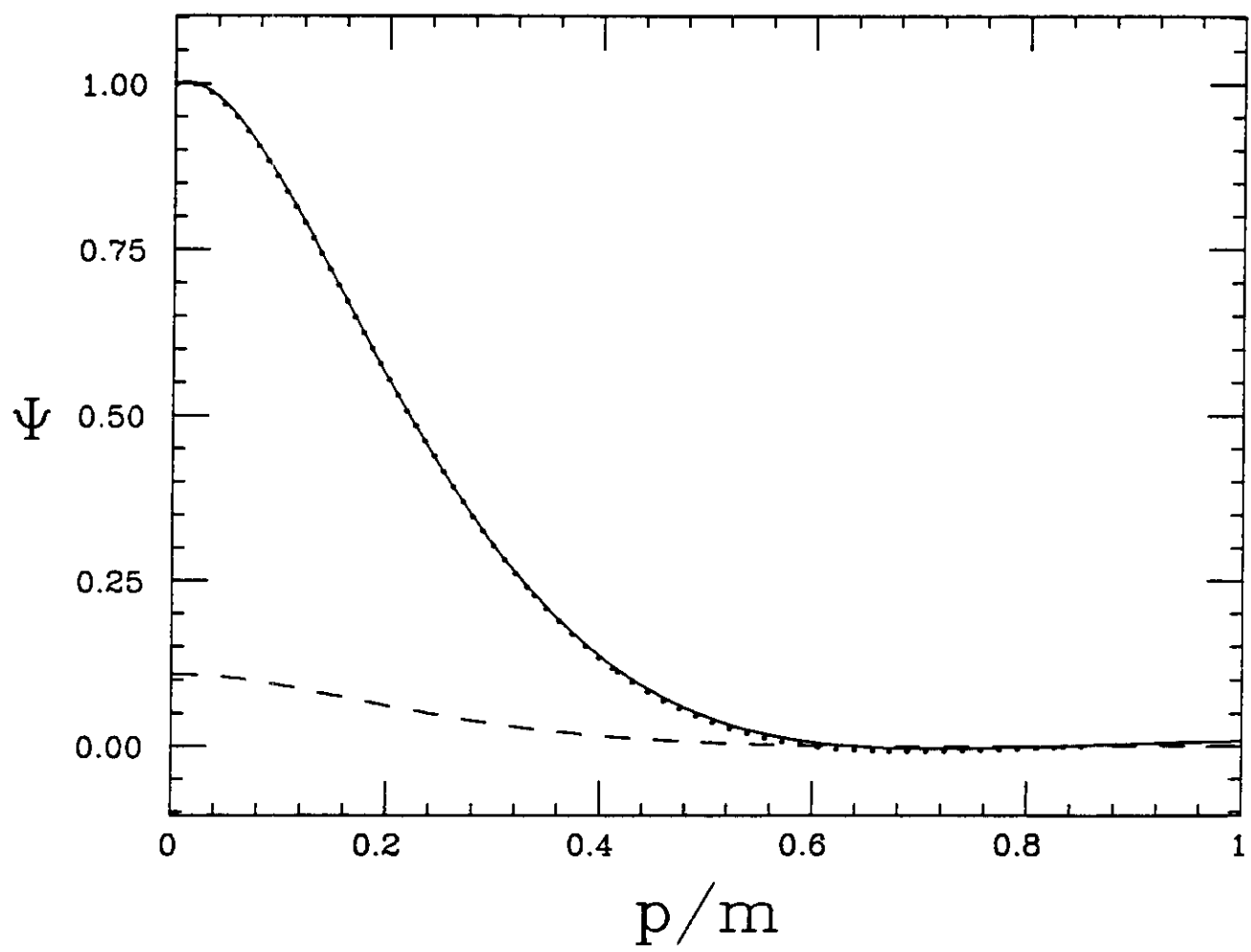
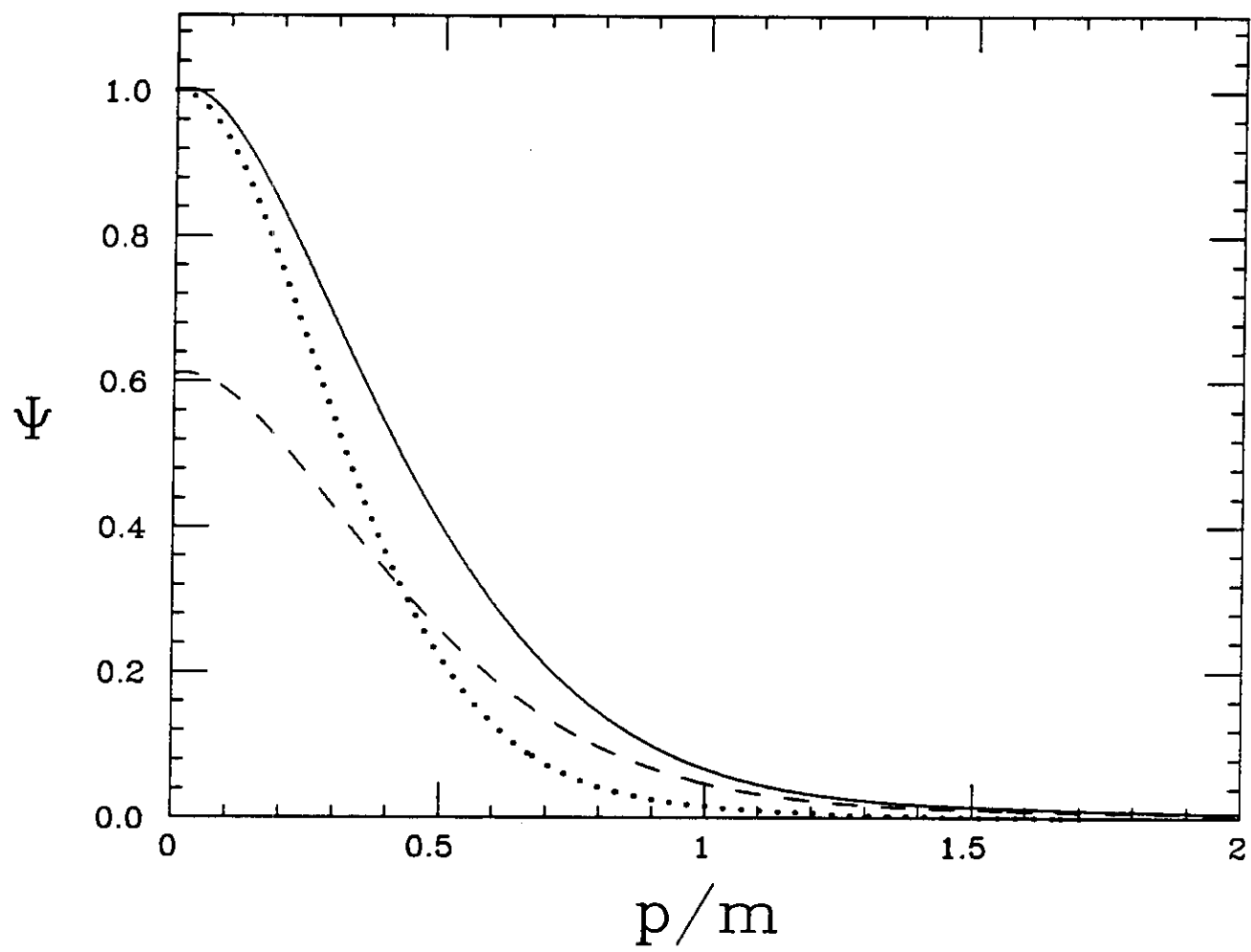


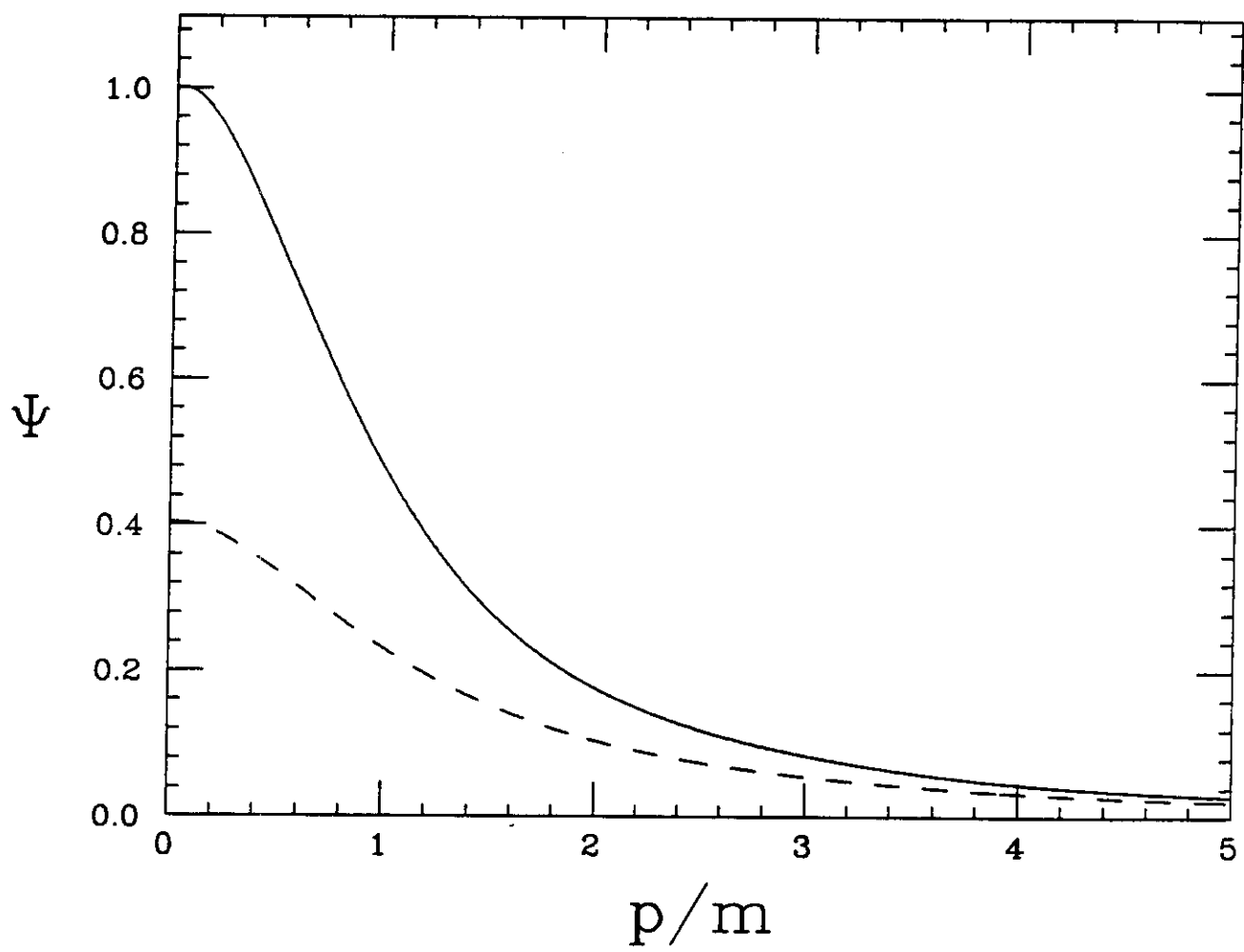
Fig. 6

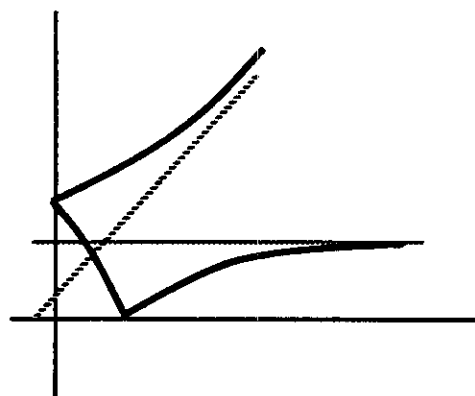




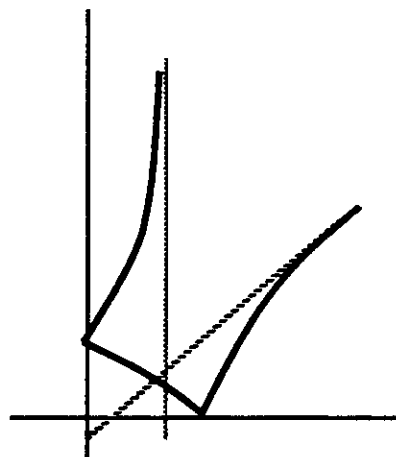




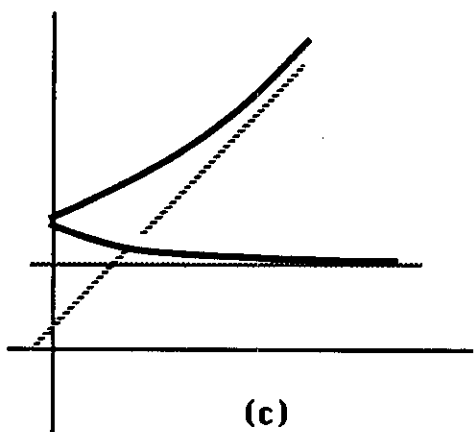




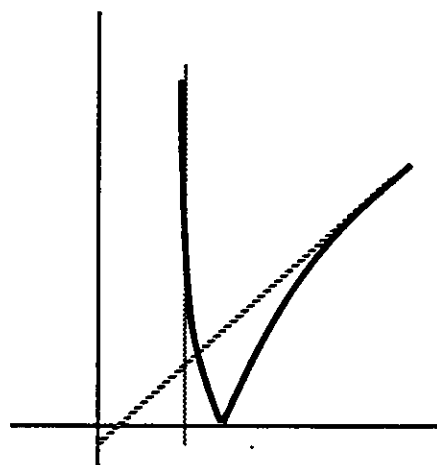
(a)



(b)



(c)



(d)

Fig. 12

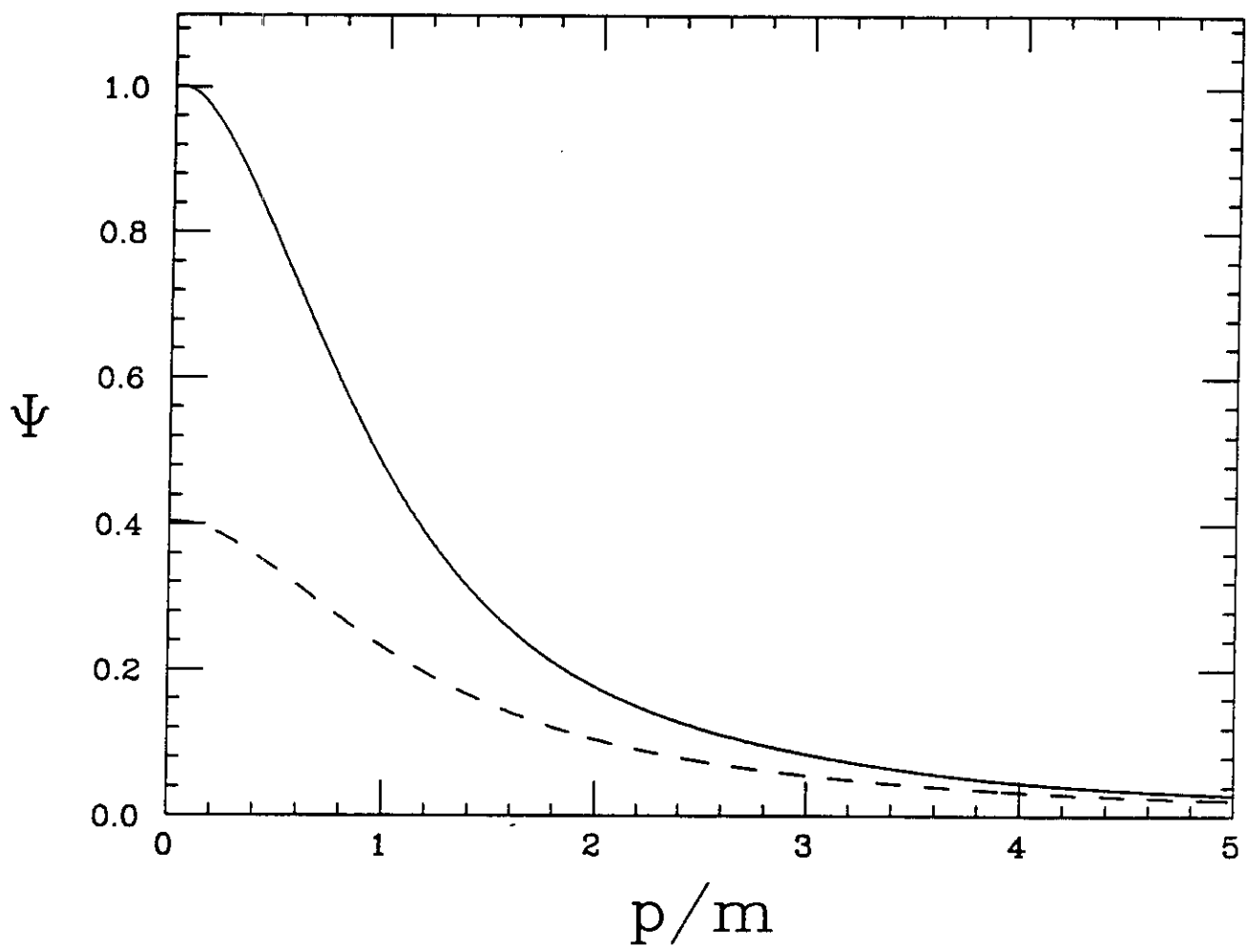


Fig. 11